marine drugs

MDPI

Article

New Polyketides and New Benzoic Acid Derivatives from the Marine Sponge-Associated Fungus *Neosartorya quadricincta* KUFA 0081

Chadaporn Prompanya [1,2], Tida Dethoup [3], Luís Gales [1,4], Michael Lee [5], José A. C. Pereira [1], Artur M. S. Silva [6], Madalena M. M. Pinto [2,7] and Anake Kijjoa [1,2,*]

1 ICBAS—Instituto de Ciências Biomédicas Abel Salazar, Universidade do Porto, Rua de Jorge Viterbo Ferreira, 228, 4050-313 Porto, Portugal; chadaporn@buu.ac.th (C.P.); lgales@ibmc.up.pt (L.G.); jpereira@icbas.up.pt (J.A.P.)
2 Interdisciplinary Centre of Marine and Environmental Research (CIIMAR), Rua dos Bragas 289, 4050-313 Porto, Portugal; madalena@ff.up.pt
3 Department of Plant Pathology, Faculty of Agriculture, Kasetsart University, 10900 Bangkok, Thailand; agrtdd@ku.ac.th
4 Instituto de Biologia Molecular e Celular (IBMC), Universidade do Porto, Rua de Jorge Viterbo Ferreira, 228, 4050-313 Porto, Portugal
5 Department of Chemistry, University of Leicester, University Road, Leicester LE 7 RH, UK; ml34@leicester.ac.uk
6 Departamento de Química & QOPNA, Universidade de Aveiro, 3810-193 Aveiro, Portugal; artur.silva@ua.pt
7 Laboratório de Química Orgânica, Departamento de Ciências Químicas, Faculdade de Farmácia Universidade do Porto, Rua de Jorge Viterbo Ferreira, 228, 4050-313 Porto, Portugal
* Correspondence: ankijjoa@icbas.up.pt; Tel.:+351-22-0428331; Fax: +351-22-2062232

Academic Editor: Russell Kerr
Received: 30 June 2016; Accepted: 12 July 2016; Published: 16 July 2016

Abstract: Two new pentaketides, including a new benzofuran-1-one derivative (**1**) and a new isochromen-1-one (**5**), and seven new benzoic acid derivatives, including two new benzopyran derivatives (**2a**, **b**), a new benzoxepine derivative (**3**), two new chromen-4-one derivatives (**4b**, **7**) and two new benzofuran derivatives (**6a**, **b**), were isolated, together with the previously reported 2,3-dihydro-6-hydroxy-2,2-dimethyl-4*H*-1-benzopyran-4-one (**4a**), from the culture of the marine sponge-associated fungus *Neosartorya quadricincta* KUFA 0081. The structures of the new compounds were established based on 1D and 2D NMR spectral analysis, and in the case of compounds **1**, **2a**, **4b**, **5**, **6a** and **7**, the absolute configurations of their stereogenic carbons were determined by an X-ray crystallographic analysis. None of the isolated compounds were active in the tests for antibacterial activity against Gram-positive and Gram-negative bacteria, as well as multidrug-resistant isolates from the environment (MIC > 256 μg/mL), antifungal activity against yeast (*Candida albicans* ATTC 10231), filamentous fungus (*Aspergillus fumigatus* ATTC 46645) and dermatophyte (*Trichophyton rubrum* FF5) (MIC > 512 μg/mL) and in vitro growth inhibitory activity against the MCF-7 (breast adenocarcinoma), NCI-H460 (non-small cell lung cancer) and A375-C5 (melanoma) cell lines (GI_{50} > 150 μM) by the protein binding dye SRB method.

Keywords: *Neosartorya quadricincta* KUFA 0081; marine-derived fungus; polyketides; pentaketides; benzoic acid derivatives; *Clathria reinwardti*

1. Introduction

Aspergillus section *Fumigati* and its teleomorph *Neosartorya* include many important species because they can be pathogenic or allergenic to man, as well as causing food spoilage and producing mycotoxins. Certain species are also found to produce interesting bioactive secondary metabolites

that can be considered to have potential for drug development [1]. For this reason, we have investigated the bioactive secondary metabolites produced from the cultures of four *Neosartorya* species collected from soil in Thailand, i.e., *Neosartorya glabra* KUFC 6311 [2], *N. pseudofischeri* KUFC 6422 [3], *N. siamensis* KUFC 6349 [4] and *N. fischeri* KUFC 6344 [5], as well as six marine-derived species of *Neosartorya*, including *N. paulistensis* KUFC 7898 [6], *N. laciniosa* KUFC 7896 [5], *N. spinosa* KUFC 8104, *N. tsunodae* KUFC 9213 [5], *N. siamensis* KUFA 0017 and *N. takakii* KUFC 7898 [7], as well as one marine-derived *Aspergillus* species (*Aspergillus similanensis* KUFA 0013) [8,9]. Recently, we have also reported the antifungal activity of the crude extract of *N. quadricincta* KUFA 0064, isolated from an agricultural soil in Southern Thailand, against plant pathogenic fungi, which are causative agents of diseases of economically-important plants of Thailand [10]. So far, the only report on secondary metabolites of *N. quadricincta* was by Ozoe et al., who described the isolation of dihydroisocoumarin derivative, PF1223, from the culture of *N. quadricincta* strain PF1223 (unidentified source). This compound was shown to inhibit the [^{3}H] EBOB binding by 65% [11]. Thus, in our ongoing search for bioactive secondary metabolites from marine-derived fungi from Thai waters, we have investigated the culture of *N. quadricincta* KUFA 0081, isolated from the marine sponge *Clathria reinwardti*, which was collected from the Coral reef at Samae San Island in the Gulf of Thailand. The ethyl acetate extract of the culture of this fungus yielded, besides the previously described 2,3-dihydro-6-hydroxy-2,2-dimethyl-4*H*-1-benzopyran-4-one (**4a**) [12], two new polyketide derivatives (**1**, **5**) and seven new benzoic acid derivatives (**2a**, **2b**, **3**, **4b**, **6a**, **6b** and **7**) (Figure 1). All of the isolated compounds were tested for their antibacterial activity against Gram-positive and Gram-negative bacteria, as well as multidrug-resistant isolates from the environment and for their antifungal activity against yeast (*Candida albicans* ATCC 10231), filamentous fungus (*Aspergillus fumigatus* ATCC 46645) and dermatophyte (*Trichophyton rubrum* FF5). Additionally, these compounds were also evaluated for their in vitro growth inhibitory activity against the MCF-7 (breast adenocarcinoma), NCI-H460 (non-small cell lung cancer) and A375-C5 (melanoma) cell lines by the protein binding dye SRB method.

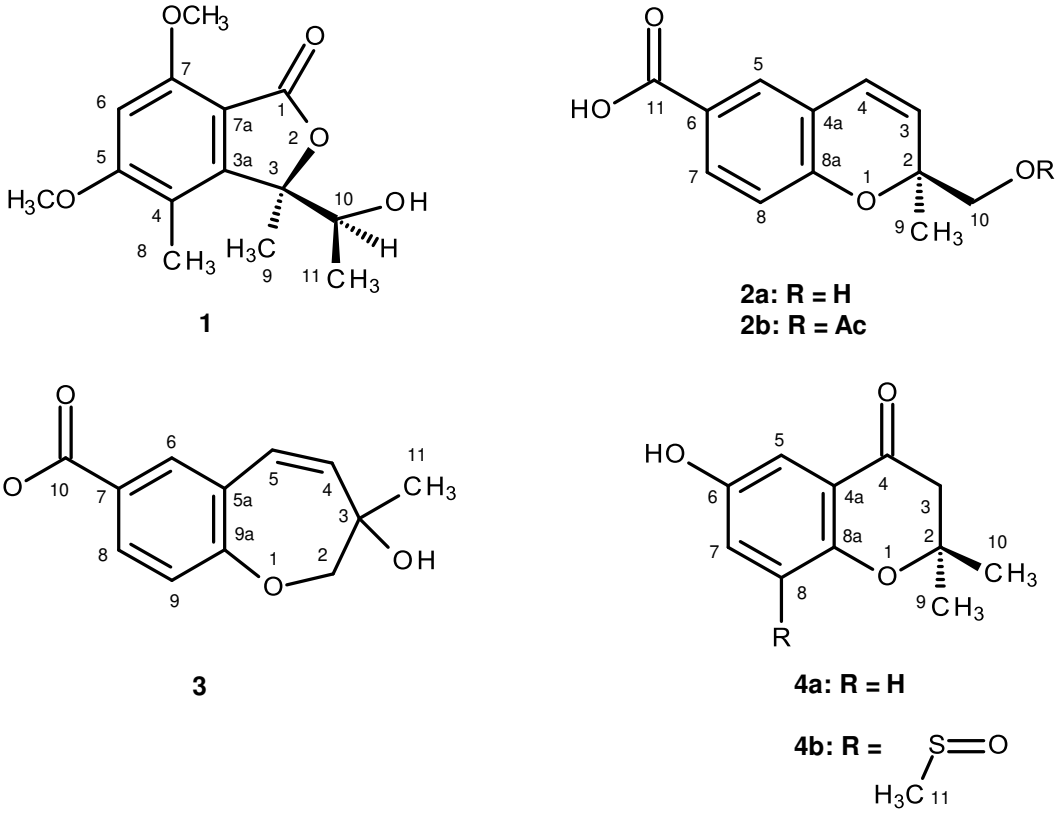

Figure 1. *Cont.*

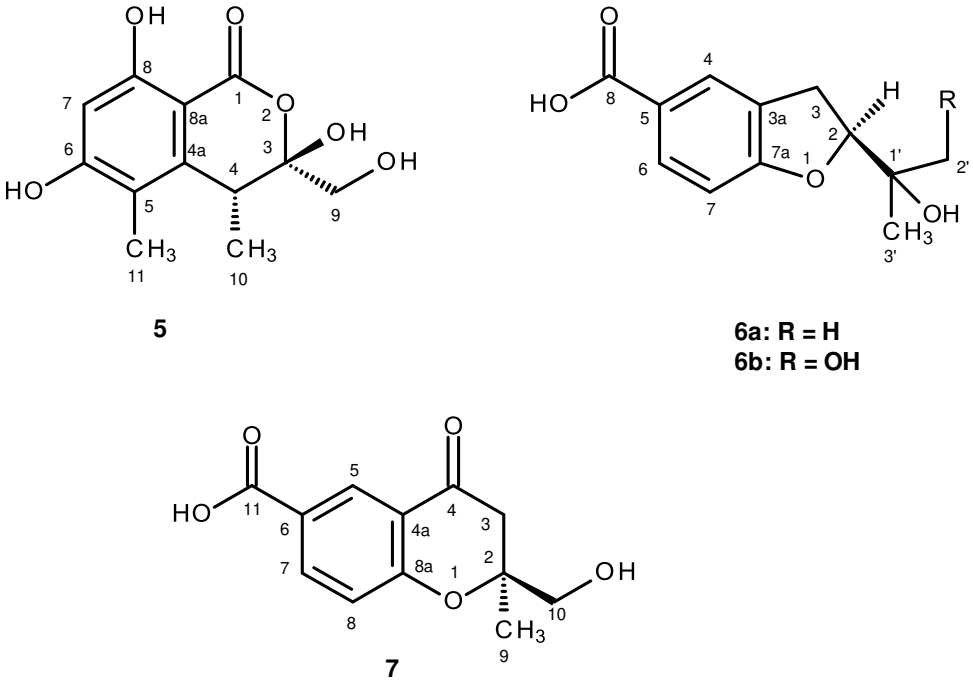

Figure 1. Secondary metabolites of *N. quadricincta* KUFA0081.

2. Results and Discussion

Compound **1** was isolated as white crystals (mp, 176–177 °C), and its molecular formula $C_{14}H_{18}O_5$ was established on the basis of the (+)-HRESIMS *m/z* 267.1243 $[M + H]^+$ (calculated 267.1332), indicating six degrees of unsaturation. The IR spectrum showed absorption bands for hydroxyl (3455 cm^{-1}), conjugated ester carbonyl (1723 cm^{-1}) and aromatic (1612, 1596 cm^{-1}) groups. The ^{13}C NMR, DEPT and HSQC spectra (Table 1, Supplementary Information, Figures S2 and S4) exhibited the signals of one conjugated ester carbonyl (δ_C 168.2), five quaternary sp^2 (δ_C 164.6, 158.3, 152.8, 111.7, 105.5), one methine sp^2 (δ_C 94.5), one oxygen bearing quaternary sp^3 (δ_C 88.8), one oxygen bearing methine sp^3 (δ_C 70.8), two methoxyl (δ_C 56.1 and 56.0) and three methyl (δ_C 21.5, 17.8 and 11.2) groups. The ^1H NMR spectrum (Table 1, Supplementary Information, Figure S1) revealed the presence of, besides a singlet of one aromatic proton at δ_H 6.41, a quartet of the oxymethine proton at δ_H 4.22 (J = 6.4 Hz), two singlets of the methoxyl groups at δ_H 3.97 s and 3.92 s, two methyl singlets at δ_H 2.12 s and 1.76 s, a methyl doublet at δ_H 0.87 (J = 6.4 Hz) and a broad band of the hydroxyl proton at δ_H 2.15. The ^1H and ^{13}C data (Table 1) revealed the presence of a pentasubstituted benzene ring. That this pentasubstituted benzene ring was part of the 5,7-dimethoxy-3,4-dimethyl-2-benzofuran-1(3*H*)-one ring system was corroborated by the HMBC correlations (Table 1, Figure 2a, Supplementary Information, Figure S5) of H-6 (δ_H 6.41, s) to C-7a (δ_C 105.3), C-4 (δ_C 111.7), C-7 (δ_C 158.3), C-5 (δ_C 164.6) and C-1 (δ_C 168.2), of OMe-5 (δ_H 3.92, s) to C-5, of OMe-7 (δ_H 3.97, s) to C-7, of H_3-8 (δ_H 2.12, s) to C-4, C-3a (δ_C 152.8) and C-5, of H_3-9 (δ_H 1.76, s) to C-3a and of the NOESY correlations of H-6 to OMe-5 and OMe-7. That another substituent of C-3 was a 1-hydroxyethyl group was supported by the COSY correlations of H-10 (δ_H 4.22, q, J = 6.4 Hz) to H_3-11 (δ_H 0.87, d, J = 6.4 Hz), by the HMBC correlations of H_3-9 to C-10 (δ_C 70.8), C-3 (δ_C 88.8) and C-3a and of H_3-11 (δ_H 0.87, d, J = 6.4 Hz) to C-3 and C-10 (Table 1, Figure 2a), as well as by the NOESY correlations of H_3-8 to H-10, H_3-9, of H_3-11 to H-10, OH-10 and of H_3-9 to H-10 (Table 1, Figure 2b, Supplementary Information, Figure S6). Final proof of the structure and the stereochemistry assigned to compound **1** was provided by its X-ray analysis (Figure 3), and since the diffraction data were collected with a Gemini PX Ultra equipped with CuKα radiation, it was possible to establish the absolute configurations of C-3 and C-10, respectively, as 3*R* and 10*S*. Since **1** is a new compound, we have named it quadricinctone A.

Table 1. ^{1}H and ^{13}C NMR ($CDCl_3$, 300.13 MHz and 75.4 MHz), HMBC and NOESY assignments for **1**.

Position	δ_C, type	δ_H, (*J* in Hz)	HMBC	NOESY
1	168.2, CO	-		
3	88.8, C	-		
3a	152.8, C	-		
4	111.7, C	-		
5	164.6, C	-		
6	94.5, CH	6.41, s	C-1, 4, 5, 7, 7a	OMe-5, 7
7	158.3, C	-		
7a	105.3, C	-		
8	11.2, CH_3	2.12, s	C-3a, 4, 5, 7	H-9, 10
9	21.5, CH_3	1.76, s	C-3, 3a, 10	H-8, 9
10	70.8, CH	4.22, d (6.4)	C-11	H-8, 9, 10
11	17.8, CH_3	0.87, d (6.4)	C-3, 10	H-10
OMe-5	56.1, CH_3	3.92, s	C-5	H-6
OMe-7	56.0, CH_3	3.97, s	C-7	H-6
OH-10	-	2.15, br	-	H-11

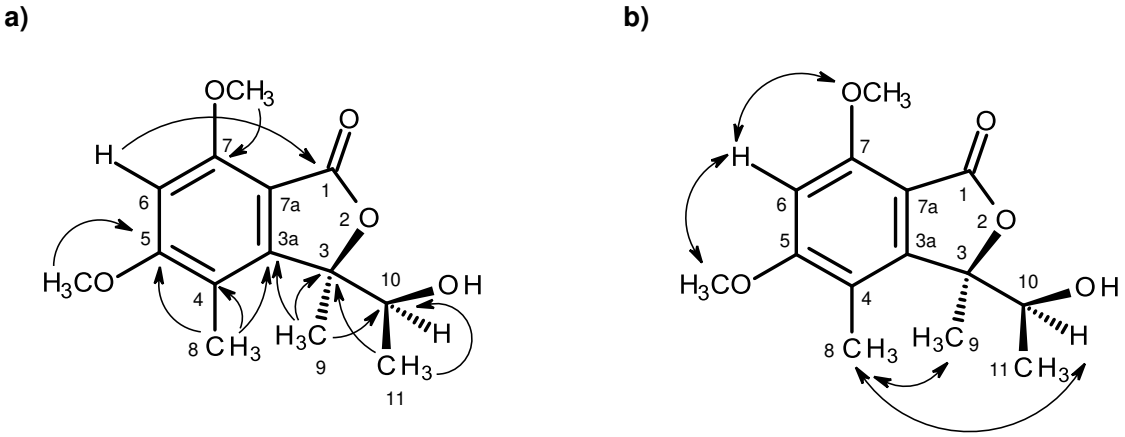

Figure 2. Key HMBC (→) (**a**) and NOESY (↔) (**b**) correlations for compound **1**.

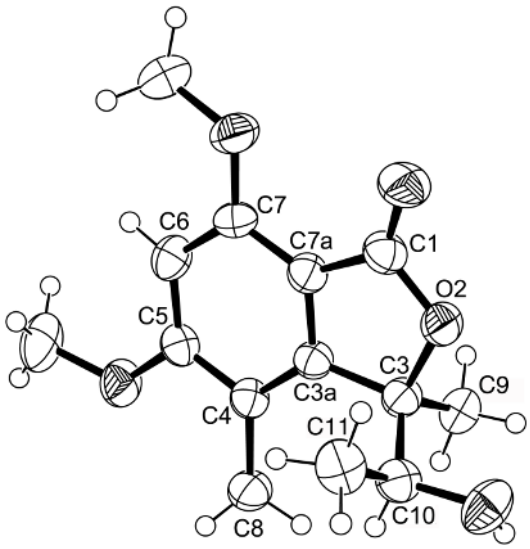

Figure 3. ORTEP diagram of compound **1**.

Compound **2a** was also isolated as white crystals (mp. 147–148 °C), and its molecular formula $C_{12}H_{12}O_4$ was determined based on the (+)-HRESIMS *m/z* 221.0820 $[M + H]^+$ (calculated 221.0814), indicating seven degrees of unsaturation. The IR spectrum showed absorption bands for hydroxyl (3447 cm^{-1}), a conjugated carbonyl (1696 cm^{-1}), aromatic (1609 cm^{-1}) and olefin (1647 cm^{-1}) groups. The ^{13}C NMR, DEPT and HSQC spectra (Table 2, Supplementary Information, Figures S8 and S10) exhibited the signals of one conjugated carboxyl carbonyl (δ_C 167.0), three quaternary sp^2 (δ_C 156.8, 123.0, 120.5), five methine sp^2 (δ_C 130.8, 128.6, 127.9, 122.8, 115.7), one oxy-quaternary sp^3 (δ_C 80.5), one oxymethylene sp^3 (δ_C 67.1) and one methyl (δ_C 23.3) groups. The ^1H NMR spectrum (Table 2, Supplementary Information, Figures S7) revealed, besides the presence of three aromatic protons of the 1,2,4 trisubstituted benzene ring at δ_H 6.79, d (*J* = 8.4 Hz), 7.65, d (*J* = 2.1 Hz) and 7.69, dd (*J* = 8.4, 2.1 Hz), two doublets of the protons of a *cis*-double bond at δ_H 6.56, d (*J* = 10.0 Hz) and 5.74, d (*J* = 10.0 Hz), a methyl singlet at δ_H 1.31, a singlet of two protons at δ_H 3.46 and two broad signals of the hydroxyl protons at δ_H 12.59 and 5.07, respectively. The COSY spectrum (Table 2, Figure 4a, Supplementary Information, Figures S9) exhibited cross-peaks of H-4 (δ_H 6.56, d, *J* = 10.0 Hz) to H-3 (δ_H 5.74, d, *J* = 10.0 Hz), of H-7 (δ_H 7.69, dd, *J* = 8.4, 2.1 Hz) to H-5 (δ_H 7.65, d, *J* = 2.1 Hz) and H-8 (δ_H 6.79, d, *J* = 8.4 Hz), confirming the presence of the 1,2,4 trisubstituted benzene ring and the *cis*-double bond. That the 1,2,4-trisubsituted benzene ring and the *cis*-double bond were part of the 2*H*-chromene-6-carboxylic acid moiety was corroborated by the HMBC correlations (Figure 4a, Supplementary Information, Figures S11) of H-5 to C-4 (δ_C 122.8), C-7 (δ_C 130.8), C-8a (δ_C 156.8) and C-11 (δ_C 167.0), of H-7 to C-5 (δ_C 127.9), C-8a, C-11, of H-8 to C-4a (δ_C 120.5), C-6 (δ_C 123.0) and C-8a, as well as of H-3 to C-4a and of H-4 to C-4a, C-5 and C-8a. As the HMBC spectrum also exhibited correlations of the methyl singlet at δ_H 1.31 (H_3-9) to C-3, C-2 (δ_C 80.5) and C-10 (δ_C 67.1) and of the singlet at δ_H 3.46 (H-10) to C-2, C-3 and CH_3-9 (δ_C 23.3), the methyl and hydroxymethyl groups were placed on C-2. The NOESY correlations (Figure 4b, Supplementary Information, Figures S12) of H-4 to H-3 and H-5, of H-3 to H-4, H_3-9 and H_2-10, of H-8 to H-7, H_2-10 and H_3-9 and of H_3-9 to H-8, H-10 also confirmed this hypothesis. Since compound **2a** was obtained in a suitable crystal, X-ray analysis was carried out, and the ORTEP view shown in Figure 5 revealed that the absolute configuration of C-2 is *S*. A literature search indicated that **2a** has never been previously reported; therefore, it was named quadricinctapyran A.

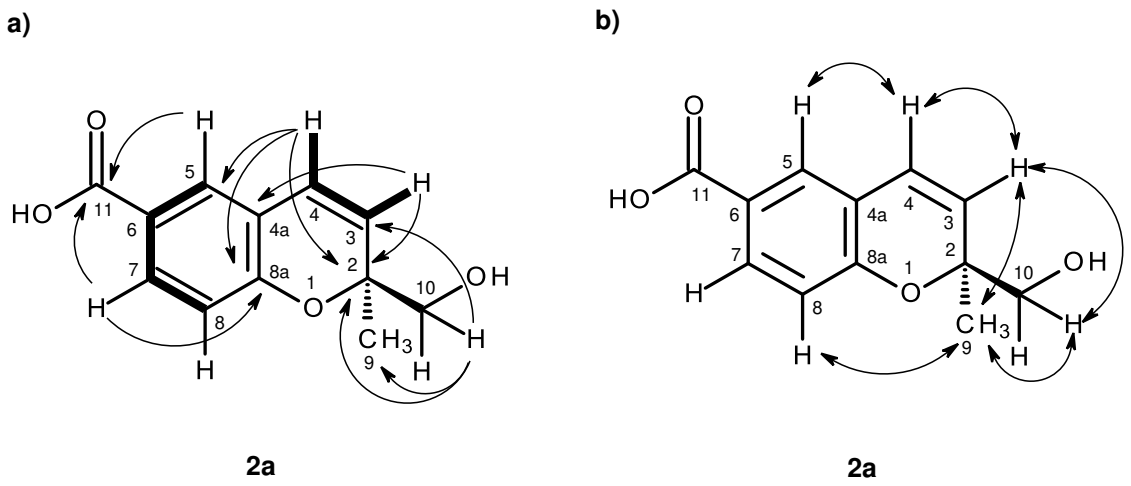

Figure 4. Key COSY (–), HMBC (→) (**a**) and NOESY (↔) (**b**) correlations for compound **2a**.

Table 2. ^{1}H and ^{13}C NMR (DMSO, 300.13 MHz and 75.4 MHz) for **2a** and **2b**.

Position	2a				2b			
	δ_C, type	δ_H, (*J* in Hz)	COSY	HMBC	δ_C, type	δ_H, (*J* in Hz)	COSY	HMBC
2	80.5, C	-			78.5, C	-		
3	128.6, CH	5.74, d (10.0)	H-4	C-2, 4a, 5, 9, 10	126.2, CH	5.59, d (10.0)	H-4	C-2, 4a, 10
4	122.8, CH	6.56, d (10.0)	H-3	C-2, 5, 8a	124.3, CH	6.51, d (10.0)	H-3	C-2, 5, 8a
4a	120.5, C	-			120.2, C	-		
5	127.9, CH	7.65, d (2.1)	H-7	C-4, 8a, 11	128.9, CH	7.75, d (2.1)	H-7	C-4, 7, 8a, 11
6	123.0, C	-			122.0, C	-		
7	139.8, CH	7.69, dd (8.4, 2.1)	H-5, 8	C-5, 8a, 11	132.2, CH	7.90, dd (8.5, 2.1)	H-5, 8	C-5, 8a, 11
8	115.7, CH	6.79, d (8.4)	H-7	C-4a, 6, 8a	116.1, CH	6.83, d (8.5)	H-7	C-4a, 6, 8a
8a	156.8, C	-			157.8, C	-		
9	23.3, CH_3	1.31, s	-	C-2, 3, 10	24.0, CH_3	1.48, s	-	C-2, 3, 10
10	67.1, CH_2	3.45, s	-	C-2, 3, 9	68.8, CH_2	4.13, d (11.7)	H-10	C-2, 3, 9
						4.24, d (11.7)	H-10	C-2, 3, 9
11	167.0, CO	-			171.7, CO	-		
OH-10	-	5.07, br	-		-	-		
OH-11	-	12.59, br	-		-	12.79, br	-	
OAc	-				170.8, CO	-		
					20.7, CH_3	1.98, s	-	CO (Ac)

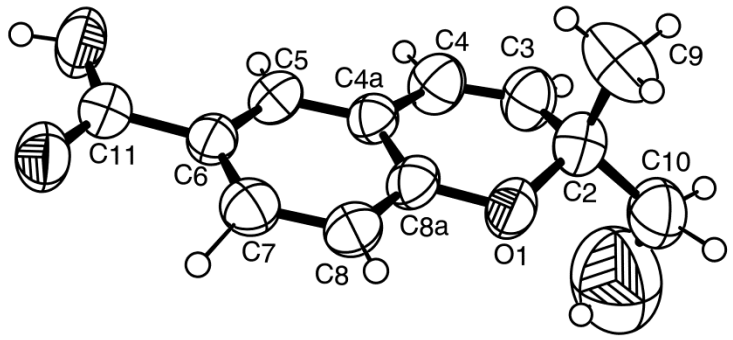

Figure 5. ORTEP diagram of compound **2a**.

Compound **2b** was isolated as a white solid (mp. 118–119 °C), and its molecular formula $C_{14}H_{14}O_5$ was established on the basis of the (+)-HRESIMS *m/z* 263.0971 $[M + H]^+$ (calculated 263.0919), indicating eight degrees of unsaturation. The ^1H and ^{13}C NMR spectral features (Supplementary Information, Figures S13 and S14) of compound **2b** resembled those of compound **2a**, except for an additional carbonyl carbon at δ_C 170.8 and a methyl group at δ_C 20.7 (δ_H 1.98, s), characteristic of the acetoxyl group (Table 2). Moreover, since the signals of the oxymethylene protons (H_2-10) of compound **2b** appeared as two doublets at δ_H 4.13 (J = 11.7 Hz) and 4.24 (J = 11.7 Hz), ca. 0.7 ppm higher than that of H_2-10 in compound **2a**, it was clear that the acetoxyl group was on C-10. This was also corroborated by the HMBC correlations (Table 2, Figure 6a, Supplementary Information, Figure S17) of H_2-10 and the methyl singlet at δ_H 1.98 to the carbonyl of the acetoxyl group (δ_C 170.8). Since Compound **2b** could not be obtained as a suitable crystal for X-ray analysis, the absolute configuration of its C-3 could not be determined with certainty. However, as compound **2b** is the acetate derivative of compound **2a**, it was speculated that the stereochemistry of its C-2 should be the same as that of C-2 of compound **2a**, i.e., 2*S*. In order to confirm this hypothesis, the NOESY experiments were carried out. The NOESY spectrum of compound **2b** showed a weak correlation of H-8 to H_3-9 and not to H_2-10 (Figure 6b, Supplementary Information, Figure S18), similar to what has been observed for compound **2a**. Acid hydrolysis of **2b** gave the product whose structure was confirmed as **2a** by ^1H and ^{13}C NMR data, as well as the optical rotation. Therefore, the absolute configuration of C-2 of **2b** is assigned as 2*S*. Compound **2b** is also a new compound, thus we named it quadricinctapyran B.

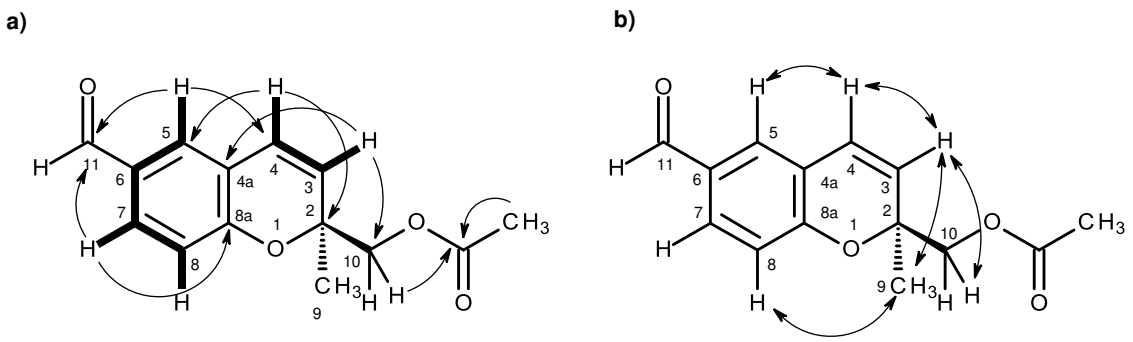

Figure 6. Key COSY (–), HMBC (→) (**a**) and NOESY (↔) (**b**) correlations for compound **2b**.

The molecular formula $C_{12}H_{12}O_4$ of compound **3**, a white solid (mp 189–191 °C), was established based on the (+)-HRESIMS *m/z* 221.0819 $[M + H]^+$ (calculated 221.0814), and thus, it is an isomer of compound **2a**. Furthermore, the general features of its ^1H and ^{13}C NMR spectra resembled those of compound **2a**. However, the chemical shift values of some of the proton and carbon signals were slightly different from those observed in compound **2a**. The ^{13}C NMR, DEPT and HSQC spectra (Table 3, Supplementary Information, Figures S20 and S22) exhibited the signals of one conjugated

carboxyl carbonyl (δ_C 166.7), three quaternary sp^2 (δ_C 161.2, 125.3, 125.0), five methine sp^2 (δ_C 139.5, 134.6, 129.8, 123.5, 119.8), one oxy-quaternary sp^3 (δ_C 70.7), one oxymethylene sp^3 (δ_C 77.0) and one methyl (δ_C 26.1) groups. The ^{1}H NMR spectrum (Table 3, Supplementary Information, Figure S19) revealed the existence of three aromatic protons of the 1,2,4-trisubstituted benzene ring, similar to that of compound **2a**, at δ_H 7.05, d (J = 8.4 Hz), 7.74, dd (J = 8.4, 2.1 Hz), 7.89, d (J = 2.1 Hz), two olefinic protons of the *cis*-double bond at δ_H 5.95, dd (J = 12.0, 1.2 Hz) and 6.31, d (J = 12.0 Hz), two oxymethylene protons at δ_H 3.84, d (J = 11.1 Hz) and 4.02, dd (J = 11.1, 1.6 Hz), and a methyl singlet at δ_H 1.26. That the carboxylic acid functionality was on C-7, and the substituent with a *cis*-double bond was on C-5a was substantiated by the HMBC correlations of H-6 (7.89, d, J = 2.1 Hz) to C-10 (δ_C 166.7), C-9a (δ_C 161.2), C-8 (δ_C 129.8) and C-5 (δ_C 123.5), of H-5 (δ_H 6.31, d, J = 12.0 Hz) to C-6 (δ_C 134.5) and C-9a and of H-4 (δ_H 5.95, dd, d, J = 12.0, 1.2 Hz) to C-5a (δ_C 125.0) (Table 3 and Figure 7a, Supplementary Information, Figure S23). However, contrary to compound **2a**, compound **3** showed the HMBC correlations of H$_2$-2 (δ_H 3.84, d, J = 11.1 Hz and 4.02, dd, J = 11.1, 1.6 Hz) to not only C-4 (δ_C 139.5), but also to C-9a (Table 3 and Figure 7a). Consequently, the benzoic acid moiety was fused with the 2,3,6,7-tetrahydro-oxepine ring through C-5a and C-9a. That the methyl group and the hydroxyl group were on C-3 of the oxepin ring was confirmed by the HMBC correlations of the methyl singlet at δ_H 1.26 (H-11) to C-3 (δ_C 70.7), C-2 (δ_C 77.0) and C-4, as well as of H$_2$-2 to C-11 (δ_C 26.1) and C-3 (Table 3 and Figure 7). This was also corroborated by the NOESY correlations of H$_3$-11 to OH-3 (δ_H 3.39, br), H$_2$-2 and H-4 (Table 3 and Figure 7b, Supplementary Information, Figure S24). Therefore, Compound **3** was identified as 3-hydroxy-3-methyl-2,3-dihydro-1-benzoxepine-7-carboxylic acid.

Table 3. ^{1}H and ^{13}C NMR (DMSO, 300.13 MHz and 75.4 MHz) and HMBC assignment for **3**.

Position	δ_C, type	δ_H, (J in Hz)	COSY	HMBC	NOESY
2α	77.0, CH$_2$	3.84, d (11.1)	H-2β	C-3, 4, 9a, 11	H-2β, 4 (w), 11 (w)
β		4.02, dd (11.1, 1.6)	H-2α	C-3, 4, 9a, 11	H-2α, 4 (w), 11 (str)
3	70.7, C	-			
4	139.5, CH	5.95, dd (12.0, 1.2)	H-5	C-2, 5a	H-2α (w), 5, 9 (w), 11
5	123.5, CH	6.31, d (12.0)	H-4	C-3, 5a, 6, 9a	H-4, 6 (str)
5a	125.0, C	-			
6	134.5, CH	7.89, d (2.1)	H-8	C-5, 8, 9a, 10	H-5
7	125.3, C	-			
8	129.8, CH	7.74, dd (8.4, 2.1)	H-6, 9	C-6, 9a	H-9
9	119.8, CH	7.05, d (8.4)	H-8	C-5a, 7, 9a	H-8
9a	161.2, C	-			
10	166.7, C	-			
11	26.1, CH$_3$	1.26, s	-	C-2, 3, 4	H-2α (w), 2β (str)
OH-3	-	3.39, br	-		H-4, 11
COOH	-	12.79, br	-		

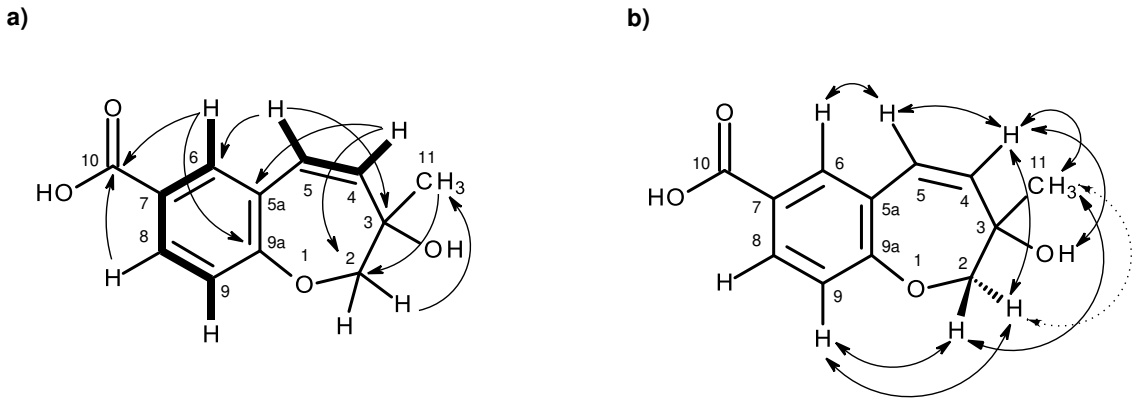

Figure 7. Key COSY (–), HMBC (→) (**a**) and NOESY (↔) (**b**) correlations for compound **3**.

As compound **3** could not be obtained as a suitable crystal for X-ray analysis, an effort to tentatively determine the relative configuration of the stereogenic carbon (C-3) by molecular mechanics conformation analysis and the NOESY experiments was carried out. Stochastic conformational search on the computational models of the structure of **3** with C-3 in *R* configuration, followed by energy minimization, converged to two half-chair conformations for the seven-membered ring C1 and C2, as depicted in Figure 8, regardless of the modelling level of the theory used (MP2/6-311G, PM3, MMFF and MM2). All methods, except for PM3, also agree that conformation C2, with the methyl group in the equatorial position, is more stable by ca. 2 kcal/mol. However, this difference can be attributed to a weak intramolecular hydrogen bond in conformation C2, between HO-3 and O-1, which is not possible in conformation C1. The semi-empirical PM3 method gives less weight to non-ideal intramolecular hydrogen bonds, as compared to the other methods, and assigns virtually the same energy to both conformations of **3**, while still orienting HO-3 towards the seven-membered ring. Since DMSO solvent molecules compete for HO-3 hydrogen bonding, it is more likely that the intramolecular bond is not an important feature of ring conformation C2 and that, in reality, both conformations have approximately the same energy.

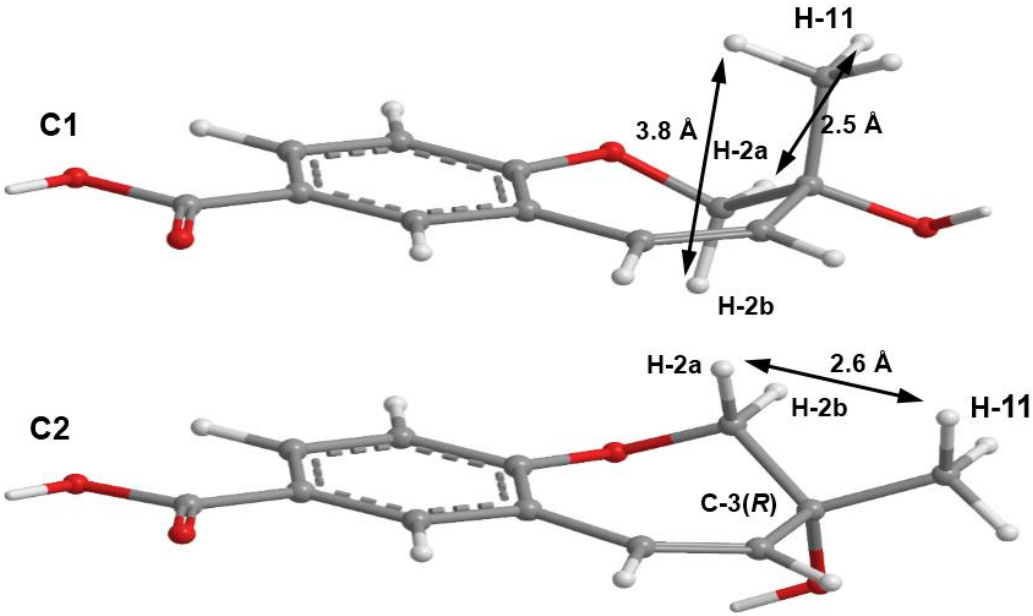

Figure 8. The two minimal energy conformations, C1 and C2, for the structure of **3**, with *R* configuration for C-3. All calculated distances and energies are exactly the same for the pairs 3*R*-C1/3*S*-C2 and 3*R*-C2/3*S*-C1. The shorter predicted inter-hydrogen distances H-2/H-11 are presented; for a discussion of the average, NOE effective distances, please refer to the main text.

Both model conformations of **3** predict hydrogen-hydrogen distances that are similar to within 0.2 Å, with the exception of some distances to the methyl group (H_3-11). The most notable are to the diastereotopic hydrogens (H_2-2), partially presented in Figure 8. While both conformations show almost the same distance between H-2a and H-11, a difference is predicted between H-2b and H-11 if the conformation C1 predominates, which should be apparent in the build-up rate of NOESY cross-peaks for small mixing times. Alternatively, the predominance of the conformation C2 would be indicated by two equal strength cross-peaks for H-2a and H-2b in cross-relaxation with H-11. It is observed that the H-2b (δ_H 3.84, d, J = 11.1 Hz)/H-11 NOESY cross-peak is weak while the H-2a

(δ_H 4.02, dd, J = 11.1, 1.6 Hz)/H-11 is medium, suggesting that the conformation C1 predominates. NOE effective distances, r_{eff}, are calculated by [13] :

$$r_{eff} = \left(\frac{1}{3}\sum_i r^{-6}_{H-2/H-10_i}\right)^{-1/6}$$

The average effective positions of the three methyl H-11$_i$ protons are relative to H-2a or H-2b. The predicted ratio r_{eff} (H-2a/H-11)/r_{eff} (H-2b/H-11) is 1.40 (1.36, if r^{-3} averages are used instead of r^{-6}). Assuming that the cross-relaxation rate is similar in both cases, the NOE intensities should also have a similar ratio [14]. Since the observed intensities ratio is actually closer to two, the evidence points towards the predominance of the conformation C1. Since, as stated previously, both conformations have similar conformational energy, the higher stability of 3*R*-C1 of **3** (or of its stereoisomer 3*S*-C2) must originate from the ready interaction of the equatorial HO-3 with the hydrogen-bonding solvent and also from a higher entropic rotational freedom of the hydroxyl and methyl groups. The NOESY spectrum also revealed the correlations of both H_2-2 to H-9. However, only one of the H_2-2, i.e., the doublet at δ_H 3.84 (J = 11.1 Hz), showed a weak cross-peak to H-4, while the double doublet at δ_H 4.02 (J = 11.1, 1.6 Hz) did not give any cross-peak to H-4. This observation led to the conclusion that the plucked oxepin ring should adopt the conformation in which H-2 at δ_H 3.84 is near H-4, i.e., in the α (axial), while H-2 at δ_H 4.02 is in β (equatorial) positions, which is in agreement with our conformational analysis. A literature search revealed that compound **3** is also a new compound, so we named it quadricinctoxepine.

Compound **4b** was isolated as white crystals (mp, 227–228 °C), and its molecular formula $C_{12}H_{14}O_4S$ was established on the basis of the (+)-HRESIMS *m/z* 255.0694 $[M + H]^+$ (calculated 255.0691). The IR spectrum showed absorption bands for hydroxyl (3442 cm^{-1}), conjugated ketone carbonyl (1690 cm^{-1}) and aromatic (1622 cm^{-1}) groups. The ^{13}C NMR, DEPT and HSQC spectra (Table 4, Supplementary Information, Figures S26 and S28) exhibited the signals of one conjugated ketone carbonyl (δ_C 191.2), four quaternary sp^2 (δ_C 151.6, 147.4, 135.7, 120.8), two methine sp^2 (δ_C 118.0, 112.4), one oxy-quaternary sp^3 (δ_C 80.9), one methylene sp^2 (δ_C 48.0) and three methyl (δ_C 40.8, 26.1 and 25.7) groups. The ^1H NMR spectrum (Table 4, Supplementary Information, Figure S25) exhibited, besides a broad singlet of the phenolic hydroxyl group at δ_H 9.85, the signals of two *meta*-coupled aromatic protons at δ_H 7.17, d (J = 3.1 Hz) and δ_H 7.35, d (J = 3.1 Hz), two geminally-coupled methylene protons at δ_H 2.80, d (J = 16.6 Hz) and 2.82, d (J = 16.6 Hz) and three methyl singlets at δ_H 1.38, s, 1.39, s, and 2.77, s. The chemical shift value of the methyl singlet at δ_H 2.77, s (δ_C 40.8), indicated that it was on the electron-withdrawing moiety. That compound **4b** was a 2,2,6,8-tetrasubstituted 2,3-dihydro-4*H*-chromen-4-one derivative was supported by the HMBC correlations of H-5 (δ_H 7.17, d, J = 3.1 Hz) to C-4 (δ_C 191.2), C-7 (δ_C 118.0) and C-8a (δ_C 147.4), of H-7 (δ_H 7.35, d, J = 3.1 Hz) to C-5 (δ_C 112.4), C-8 (δ_C135.7), C-8a, as well as of H-2 (δ_H 2.80, d, J = 16.6 Hz and 2.82, d, J = 16.6 Hz) to C-3 (δ_C 80.9) and C-4 (Table 4, Figure 9, Supplementary Information, Figure S28). As the HMBC spectrum also exhibited cross-peaks of a broad singlet of the phenolic hydroxyl proton at δ_H 9.85 to C-5, C-6 (δ_C 151.6) and C-7 and of the singlets of the methyl groups at δ_H 1.38 and 1.39 to C-2 (δ_C 48.0) and C-3, the hydroxyl group was placed on C-6, and the two methyl groups were placed on C-2. Since this partial structure accounted for only $C_{11}H_{11}O_3$, another portion of the molecule must contain CH_3SO. That the methyl sulfoxide group was on C-8 was supported by the presence of the deshielded methyl group at δ_H 2.77, s (δ_C 40.8), as well as by the HBMC cross-peak of H_3-11 (δ_H 2.77, s) to C-8. Final proof of the structure of compound **4b** was provided by its X-ray analysis, and its ORTEP view is shown in Figure 10. Moreover, the ORTEP view also revealed that the absolute configuration of the sulfoxide group in compound **4b** is *R*. A literature search showed that compound **4b** is a new compound, and thus, we have named it quadricinctone B.

Table 4. ^{1}H and ^{13}C NMR (DMSO, 300.13 MHz and 75.4 MHz) and HMBC assignment for **4b**.

Position	δ_C, type	δ_H, (*J* in Hz)	COSY	HMBC
2	80.9, C	-		
3	48.0, CH_2	2.80, d (16.6)	H-3	C-2, 4, 9, 10
		2.85, d (16.6)	H-3	C-2, 4, 9, 10
4	191.2, CO	-		
4a	120.8, C	-		
5	112.4, CH	7.17, d (3.1)	H-7	C-4, 6, 7, 8a
6	151.6, C	-		
7	118.7, CH	7.35, d (3.1)	H-5	C-5, 6, 8, 8a
8	135.7, C	-		
8a	147.4, C	-		
9	26.1, CH_3	1.39, s	-	C-2, 3, 10
10	25.7, CH_3	1.38, s	-	C-2, 3, 9
11	40.8, CH_3	2.77, s	-	C-8
OH-6	-	9.85, s		C-5, 6, 7

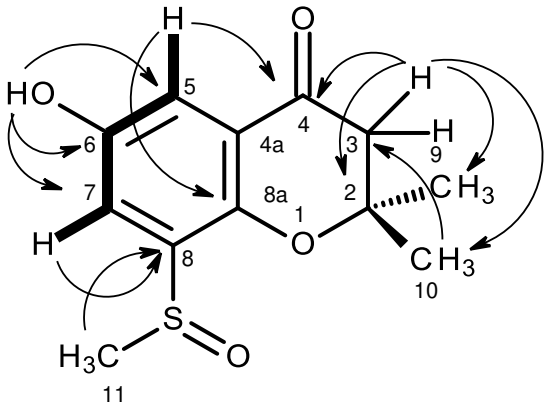

4b

Figure 9. Key COSY (–) and HMBC (→) correlations for compound **4b**.

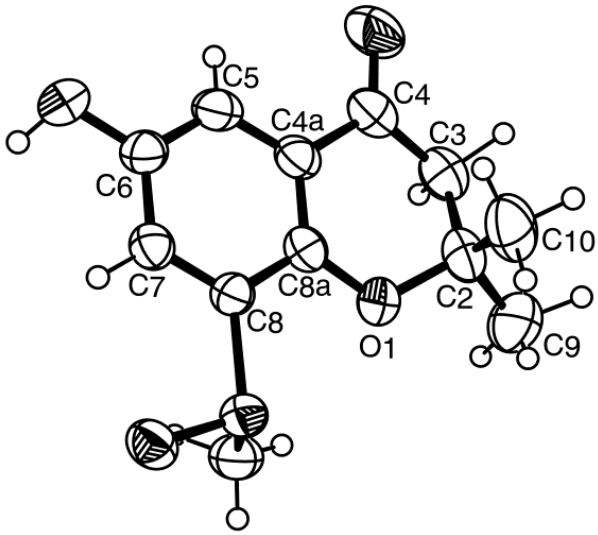

Figure 10. ORTEP diagram of compound **4b**.

The molecular formula $C_{12}H_{14}O_6$ of compound **5** was determined based on the (+)-HRESIMS *m/z* 255.0875 (calculated 255.0869), indicating six degrees of unsaturation. The IR spectrum exhibited absorption bands for hydroxyl (3439 cm^{-1}), conjugated ester carbonyl (1660 cm^{-1}) and aromatic (1643 cm^{-1}) groups. The ^{13}C NMR, DEPT and HSQC spectra (Table 5, Supplementary Information, Figures S31 and S33) exhibited the signals of one conjugated ester carbonyl (δ_C 168.8), five quaternary sp^2 (δ_C 162.9, 161.3, 144.6, 113.5, 98.9), one methine sp^2 (δ_C 99.9), one quaternary sp^3 of a hemiketal (δ_C 104.8), one methine sp^3 (δ_C 34.9), one oxymethylene sp^3 (δ_C 63.7) and two methyl (δ_C 16.3 and 9.8) carbons. The ^1H NMR spectrum (Table 5, Supplementary Information, Figure S30) exhibited, besides a singlet of one aromatic proton at δ_H 6.27, a singlet of a hydrogen-bonded phenolic hydroxyl at δ_H 11.24 and a broad signal of another phenolic hydroxyl at δ_H 10.62, two broad signals of the hydroxyl groups at δ_H 5.26 and 7.07, one broad doublet of two methylene protons at δ_H 3.65 (J = 16.6 Hz), a broad signal of one methine proton at δ_H 3.26, one methyl doublet at δ_H 1.06 (J = 7.2 Hz) and one methyl singlet at δ_H 1.98. That compound **5** was a 3,3,4,5,6,8-hexasubstituted 3,4-dihydro-1*H*-isochromen-1-one was supported by the HBMC correlations of OH-8 (δ_H 11.24, s) to C-8 (δ_C 161.3), C-7 (δ_C 99.9), C-8a (δ_C 98.9) and of H-7 (δ_H 6.27, s) to C-5 (δ_C 113.5), C-6 (δ_C 162.9), C-8 and C-8a (Table 5, Figure 11, Supplementary Information, Figure S34). Since the methyl singlet at δ_H 1.98 gave HMBC cross-peaks to C-5 and the carbons at δ_C 144.6 and 162.9 (Table 5, Figure 11), the methyl group (δ_H 1.98; δ_C 9.8) and another hydroxyl group (δ_H 10.62, br) were placed on C-5 and C-6, respectively, and the carbon signals at δ_C 144.6 and 162.9 were assigned for C-4a and C-6, respectively. On the other hand, the COSY spectrum (Table 5, Supplementary Information, Figure S32) showed cross-peaks of the broad signal at δ_H 3.26 to the methyl doublet at δ_H 1.06 (J = 7.2 Hz) and of the broad signal at δ_H 5.26 to the broad doublet at δ_H 3.65 (J = 16.6 Hz), while the HMBC spectrum (Table 5, Figure 11) gave cross-peaks of the methyl doublet at δ_H 1.06 (J = 7.2 Hz) to C-4a, C-4 (δ_C 34.9), and the signal of the quaternary carbon at δ_C 104.8 (C-3), the methyl and the hydroxymethyl substituents were placed on C-4 and C-3, respectively. Therefore, another hydroxyl group (δ_H 7.07, br) was on C-3. This was supported by the chemical shift value of C-3, which is typical for a hemiketal carbon. Since compound **5** could be obtained as a suitable crystal (mp. 223–224 °C), its X-ray analysis was performed. The ORTEP view of compound **5**, shown in Figure 12, not only confirmed the proposed structure, but also determined the absolute configuration of C-3 and C-4 as 3*S*, 4*R*. Since compound **5** is a new compound, it was named quadricinctone C.

Table 5. ^1H and ^{13}C NMR (DMSO, 300.13 MHz and 75.4 MHz) and HMBC assignment for **5**.

Position	δ_C, type	δ_H, (J in Hz)	COSY	HMBC
1	168.8, C	-		
3	104.8, C	-		
4	34.9, CH	3.26, m	H_3-10	
4a	144.6, C	-		
5	113.5, C	-		
6	162.9, C	-		
7	99.9, CH	6.27, s	-	C-1 (w), 5, 6, 8, 8a
8	161.3, C	-		
8a	98.9, C	-		
9	63.7, CH_2	3.65, brd (16.6)	OH-9	
10	16.3, CH_3	1.06, d (7.2)	H-4	C-3, 4, 4a
11	9.8, CH_3	1.98, s	-	C-4a, 5, 6
OH-3	-	7.07, br	-	
OH-5	-	10.62, br	-	
OH-8	-	11.24, s	-	C-7, 8, 8a
OH-9	-	5.26, br	-	

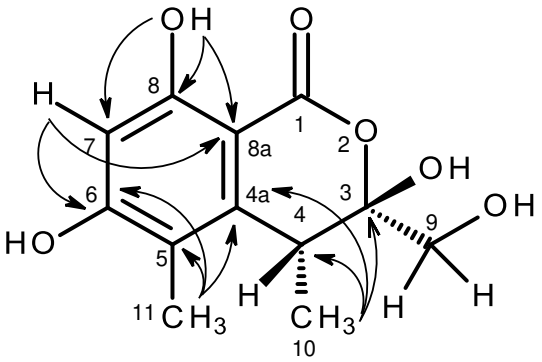

5

Figure 11. Key HMBC (→) correlations for compound **5**.

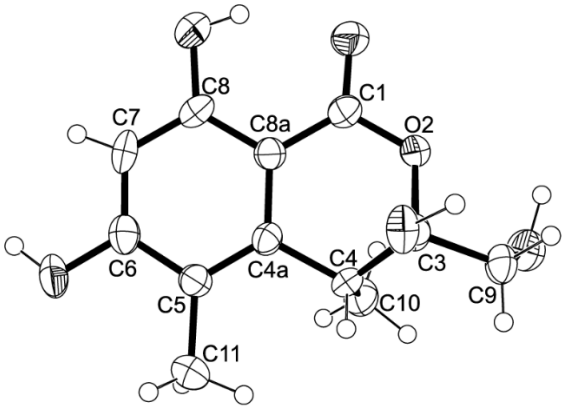

Figure 12. ORTEP diagram of compound **5**.

Compound **6a** was also isolated as white crystals (mp. 149–150 °C), and its molecular formula $C_{12}H_{14}O_4$ was determined based on the (+)-HRESIMS *m/z* 223.9067 $[M + H]^+$ (calculated 223.9070), indicating six degrees of unsaturation. The IR spectrum showed absorption bands for hydroxyl (3417 cm^{-1}), a conjugated carbonyl (1681 cm^{-1}) and aromatic (1634 cm^{-1}) groups. The ^{13}C NMR, DEPT and HSQC spectra (Table 6, Supplementary Information, Figures S36 and S38) exhibited the signals of one conjugated carboxyl carbonyl (δ_C 167.2), two quaternary sp^2 (δ_C 128.2, 122.6), one oxy-quaternary sp^2 (δ_C 163.7), three methine sp^2 (δ_C 130.4, 126.4, 108.4), one oxy-quaternary sp^3 (δ_C 70.0), one oxymethine sp^3 (δ_C 90.2), one methylene sp^2 (δ_C 29.3) and two methyl (δ_C 25.9 and 24.9) carbons. The ^1H NMR spectrum (Table 6, Supplementary Information, Figure S35) showed signals of three aromatic protons of the 1,2,4-trisubstituted benzene ring at δ_H 7.75, d (J = 1.8 Hz), 7.72, dd (J = 8.3, 1.8 Hz), 6.80, d (J = 8.3 Hz), in addition to a broad signal of the hydroxyl proton at δ_H 12.49, a triplet of one proton at δ_H 4.64 (J = 8.9 Hz), a doublet of two protons at δ_H 3.17 (J = 8.9 Hz) and two methyl singlets at δ_H 1.13 and 1.14. That the 1,2,4-trisubstituted benzene ring was part of 2,5-disubstituted 2,3-dihydro-1-benzofuran was supported by the COSY correlations of H-6 (δ_H 7.72, dd, J = 8.3, 1.8 Hz) to H-4 (δ_H 7.75, d, J = 1.8 Hz) and H-7 (δ_H 6.80, d, J = 8.3 Hz) and of H-2 (δ_H 3.17, J = 8.9 Hz) to H-3 (δ_H 4.64, J = 8.9 Hz)(Table 6, Figure 13a, Supplementary Information, Figure S37), as well as of the HMBC correlations of H-4 to C-6 (δ_C 130.4) and C-7a (δ_C 163.7), of H-6 to C-4 (δ_C 126.4), of H-3 to C-2 (δ_C 90.2), C-3a (δ_C 128.2) and C-7a and of H-7 to C-3a, C-7a and C-5 (δ_C 122.6) (Table 6, Figure 13a, Supplementary Information, Figure S39). That the carboxyl group was on C-5 was supported by the HMBC correlations of H-4 and H-6 to the conjugated carbonyl

at δ_C 167.2 (Table 6, Figure 13a), along with the presence of a broad signal at δ_H 12.49, which is characteristic of a hydroxyl group of carboxylic acid. In the same manner, that the 2-hydroxypropyl substituent was placed on C-2 was evidenced by the HMBC correlations of H-2 (δ_H 4.64, J = 8.9 Hz) to C-3 (δ_C 29.3), C-1′ (δ_C 70.0), C-2′ (δ_C 24.9), C-3′ (δ_C 25.9) (Table 6, Figure 13a), as well as by the NOESY correlations of H-2 to H-3, H_3-2′ (δ_H 1.14, s) and H_3-3′ (δ_H 1.13, s)(Figure 13b). Therefore, compound **6a** was identified as 2-(2-hydroxypropan-2-yl)-2,3-dihydro-1-benzofuran-5-carboxylic acid. A literature search revealed that compound **6a** has the same flat structure as anodendroic acid (2-(1-hydroxy-1-methylethyl)-2,3-dihydrobenzofuran-5-carboxylic acid), which was first isolated from the stem of *Anodendron affine* Durce [15]. Anodendroic acid was later synthesized by Yamaguchi et al. [16]; however, its ^{1}H NMR data (DMSO-d_6) were slightly different from those reported by Shima et al. [15]. Anodendroic acid was also obtained by basic hydrolysis of its methyl ester, a constituent of *Eriodictyon sessilifolium* [17], and also by biotransformation of 3-(γ,γ-dimethylallyl)-*p*-coumaric acid [18]. It is interesting to note that, in all of these reports, the identity of anodendroic acid was achieved by comparing its melting point, ^{1}H NMR and MS data with those reported by Shima et al. [15], while no stereochemistry of C-2 was indicated. However, when compared to the ^{1}H NMR and other physical data of compound **6a** with those reported for anodendroic acid by Shima et al. [15], it was found that the ^{1}H NMR data of anodendroic acid (in pyridine-d_6) [15] were slightly different from those of compound **6a** (in DMSO-d_6). Therefore, it was not possible to compare these ^{1}H NMR data, since they were obtained in different solvents. Interestingly, the ^{1}H NMR data, obtained in DMSO-d_6 by Yamaguchi et al. [16], were also slightly different from those of compound **6a**. The obvious differences between anodendroic acid [15] and compound **6a** are their melting points and optical rotations. While anodendroic acid (mp. 212–214 °C) is laevorotatory ($[\alpha]_D^{26}$ −19°, *c* 0.7, EtOH) [15], compound **6a** (mp. 149–150 °C) is dextrorotatory ($[\alpha]_D^{20}$ +74°, *c* 0.03, MeOH). Consequently, we concluded that the structure of compound **6a** is different from that of anodendroic acid. This fact has prompted us to investigate the stereochemistry of compound **6a**. Since Compound **6a** was obtained as a suitable crystal for X-ray diffraction, its X-ray analysis was carried out. The ORTEP view of compound **6a** shown in Figure 14 not only confirmed its proposed structure, but also revealed the absolute configuration for C-2 as 2*R*. Therefore, compound **6a** is a new compound, and we have named it quadricinctafuran A. Since anodendroic acid exhibited the opposite sign of rotation to that of compound **6a**, it is probable that the absolute configuration of its C-2 is 2*S*. This is not unusual, since fomannoxin, another 2,3-dihydrobenzofuran derivative, also showed the opposite optical rotation and has the opposite absolute configuration to tremetone, even though they have very similar structures [16].

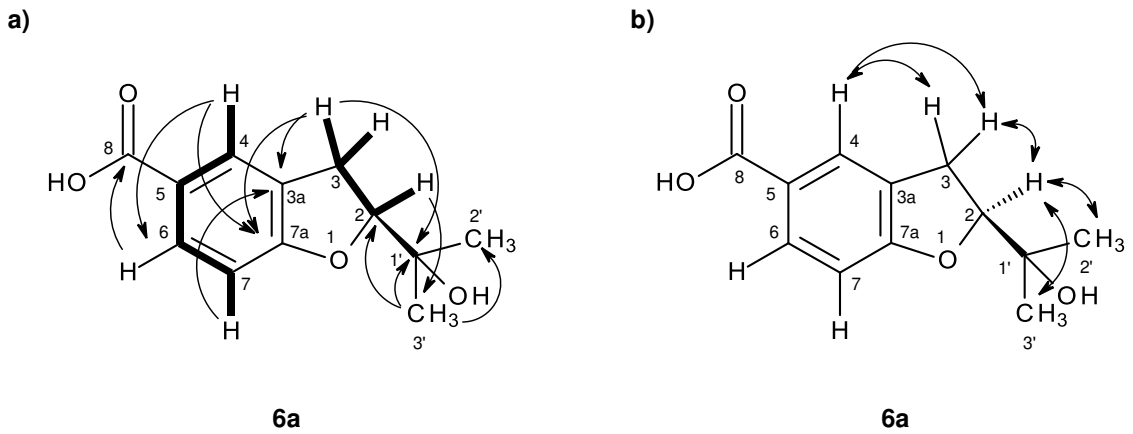

Figure 13. Key COSY (–), HMBC (→) (**a**) and NOESY (↔) (**b**) correlations for compound **6a**.

Table 6. ^{1}H and ^{13}C NMR (DMSO, 300.13 MHz and 75.4 MHz) and HMBC assignment for **6a** and **6b**.

Position	6a				6b			
	δ_C, type	δ_H, (*J* in Hz)	COSY	HMBC	δ_C, type	δ_H, (*J* in Hz)	COSY	HMBC
2	90.2, CH	4.64, t (8.9)	H-3	C-1′, 2′, 3′	86.5, CH	4.83, dd (9.7, 8.1)	H-3	
3	29.3, CH_2	3.17, d (8.9)	H-2	C-1′, 2, 3a, 7a	28.7, CH_2	3.19, m	H-2	C-1′, 3a
3a	128.2, C	-			128.4, C	-		
4	126.4, CH	7.75, d (1.8)	H-6	C-6, 7a, 8	126.4, CH	7.76, d (1.8)	H-6	C-3, 6, 7a
5	122.6, C	-			122.6, C	-		
6	130.4, CH	7.72, dd (8.3, 1.8)	H-4, 7	C-4, 7a, 8	130.8, CH	7.71, dd (8.3, 1.8)	H-4, 7	C-4, 7a, 8
7	108.4, CH	6.80, d (8.3)	H-6	C-3a, 5, 7a	108.4, CH	6.79, d (8.3)	H-6	C-3a, 5, 7a
7a	163.7, C	-			163.6, C	-		
8	167.2, C	-			167.2, C	-		
1′	70.0, C	-			72.5, C	-		
2′	24.9, CH_3	1.14, s	-	C-1′, 2, 3′	66.7, CH_2	3.33, s	-	C-1′, 2, 3′
3′	25.9, CH_3	1.13, s	-	C-1′, 2, 2′	20.0, CH_3	1.09, s		C-1′, 2, 2′
OH-8	-	12.49, br	-		-	12.47, br	-	

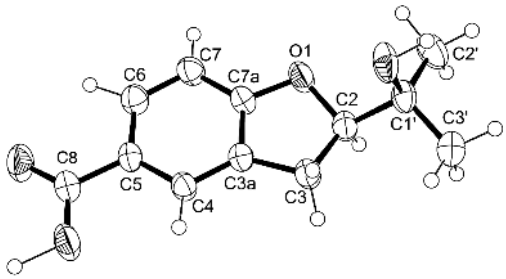

Figure 14. ORTEP diagram of **6a**.

The (+)-HRESIMS of compound **6b** gave the $[M + H]^+$ at *m/z* 239.0919 (calculated 239.0919), indicating its molecular formula $C_{12}H_{14}O_5$ and, therefore, six degrees of unsaturation. The general features of its ^1H and ^{13}C NMR spectra resembled those of compound **6a**. The ^{13}C NMR, DEPT and HSQC spectra (Table 6, Supplementary Information, Figures S42 and S44) exhibited the signals of one conjugated carboxyl carbonyl (δ_C 167.2), two quaternary sp^2 (δ_C 128.4, 122.6), one oxy-quaternary sp^2 (δ_C 163.6), three methine sp^2 (δ_C 130.8, 126.4, 108.4), one oxy-quaternary sp^3 (δ_C 72.5), one oxymethine sp^3 (δ_C 86.5), one methylene sp^2 (δ_C 28.7), one oxymethylene sp^2 (δ_C 66.7) and one methyl (δ_C 20.0) carbons. The ^1H NMR and COSY spectra (Table 6, Supplementary Information, Figures S41 and S43) showed similar proton signals of the 2,3-dihydro-1-benzofuran-5-carboxylic acid nucleus to those of **6a**. However, it exhibited only one methyl singlet at δ_H 1.09 and another singlet of oxymethylene protons at δ_H 3.33, instead of two methyl singlets as in compound **6a**. Therefore, the difference between the structures of compounds **6a** and **6b** resides in the substitutions on C-2. That the substituent on C-2 of compound **6b** was 1,2-dihydroxypropyl was evidenced by not only its molecular formula ($C_{12}H_{14}O_5$), which has one more oxygen atom than that of compound **6a** ($C_{12}H_{14}O_4$), but also the presence of the oxymethylene carbon at δ_C 66.7 (C-2′; δ_H 3.33, s). Moreover, the chemical shift value of C-2 (δ_C 86.5) was nearly 4 ppm lower than that of compound **6a** (δ_C 90.2). Thus, compound **6b** was identified as 2-(1,2-dihydroxypropan-2-yl)-2,3-dihydro-1-benzofuran-5-carboxylic acid. This was confirmed by the HMBC correlations of H_3-3′ (δ_H 1.09) to C-1′ (δ_C 72.5) and C-2′ (δ_C 66.7), as well of H_2-2′ (δ_H 3.33, s) to C-1′ (δ_C 72.5) and C-3′ (δ_C 20.0) (Figure 15, Supplementary Information, Figure S45). Since compound **6b** could not be obtained as suitable crystals for X-ray crystallography, it was not possible to determine the absolute configuration of C-2 by X-ray analysis. Moreover, as compound **6b** also has a tertiary hydroxyl group on C-1′ and a primary hydroxyl group on C-2′, it was not possible to determine the absolute configurations of C-2 and C-1′ by Mosher's method. On the other hand, since the methyl group on C-1 in compound **6a** was replaced by the hydroxymethyl group incompound **6b**, it is legitimate to postulate that compounds **6b** is derived from compound **6a**. Consequently, the absolute configuration of C-2 of compound **6b** should be the same as that of compound **6a**, i.e., 2*R*. However, it is not yet possible to determine the absolute configuration of C-1′. Compound **6b** is also a new compound, and we have named it quadricinctafuran B.

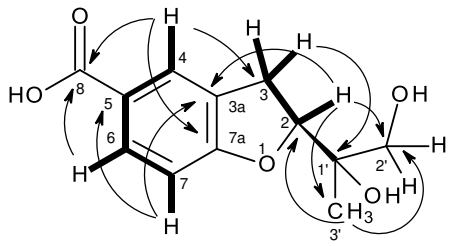

6b

Figure 15. Key COSY (–) and HMBC (→) correlations for compound **6b**.

Compound **7** was also isolated as white crystals (mp. 196–197 °C), and its molecular formula $C_{14}H_{12}O_5$ was established on the basis of the (+)-HRESIMS *m/z* 237.0792 $[M + H]^+$ (calculated 237.0763), indicating seven degrees of unsaturation. The IR spectrum showed absorption bands for hydroxyl (3404 cm^{-1}), conjugated ketone carbonyl (1708 cm^{-1}), conjugated carboxyl carbonyl (1670 cm^{-1}) and aromatic (1558, 1540 cm^{-1}) groups. The ^{13}C NMR, DEPT and HSQC spectra (Table 7, Supplementary Information, Figures S48 and S50) exhibited the signals of one conjugated ketone carbonyl (δ_C 191.1), one conjugated carboxyl carbonyl (δ_C 166.4), one oxy-quaternary sp^2 (δ_C 162.9), two quaternary sp^2 (δ_C 123.0, 119.6), three methine sp^2 (δ_C 136.4, 127.5, 118.5), one oxy-quaternary sp^3 (δ_C 83.0), one oxymethylene sp^2 (δ_C 66.8), one methylene sp^2 (δ_C 43.4) and one methyl (δ_C 21.2) carbons. The ^1H NMR spectra (Table 7, Supplementary Information, Figure S47) exhibited, besides the signals of three aromatic protons of the 1,2,4-trisubstituted benzene ring at δ_H 8.26, d (*J* = 2.3 Hz), 8.04, dd (*J* = 8.7, 2.3 Hz), 7.07, d (*J* = 8.7 Hz), a methyl singlet at δ_H 1.30, two pairs of geminally-coupled methylene protons at δ_H 2.74, d (*J* = 16.7 Hz)/3.00, d (*J* = 16.7 Hz) and δ_H 3.49, dd (*J* = 11.6, 4.5 Hz)/3.59, dd (*J* = 11.6, 4.2 Hz); the latter showed COSY correlations with the broad triplet of the hydroxyl proton at δ_H 5.26 (Table 7, Figure 16a, Supplementary Information, Figure S49). As the HMBC spectrum exhibited correlations of the aromatic proton signal at δ_H 8.26, d (*J* = 2.3 Hz, H-5) to the oxy-quaternary sp^2 carbon at δ_C 162.9 (C-8a), as well as to the conjugated ketone carbonyl carbon at δ_C 191.1 (C-4) and the methine sp^2 at δ_C 136.4 (C-7) (Table 7, Figure 16a, Supplementary Information, Figure S51), the ketone moiety was placed on C-4a. Additionally, the HMBC spectrum also showed correlations of H-8 (δ_H 7.07, d, *J* = 8.7 Hz) to C-8a and the quaternary sp^2 carbons at δ_C 123.0 and 119.6; they were therefore assigned to C-4a and C-6, respectively (Table 7, Figure 16a). The presence of the 1-hydroxy-2-methyl-2-oxypropyl moiety was supported by the HMBC correlations of the methyl singlet at δ_H 1.30 (CH_3-9) to the oxy-quaternary sp^3 carbon at δ_C 83.0 (C-2), the oxymethylene sp^3 carbon at δ_C 66.8 (C-10) and the methylene sp^3 carbon at δ_C 43.4 (C-3), as well as of the H_2-3 (δ_H 2.74, d, *J* = 16.7 Hz/3.00, d, *J* = 16.7 Hz) to C-2, C-9 (δ_C 21.2) and C-10 (Table 7, Figure 16a). Since H_2-3 also gave a HMBC cross-peak to C-4, the 1-hydroxy-2-methyl-2-oxypropyl moiety was linked to C-4. Due to the fact that these two moieties accounted for only $C_{11}H_{12}O_4$, it was concluded that the carboxyl group (δ_C 166.4, δ_H 12.69 br) was on C-6. Therefore, compound **7** was identified as 2-(hydroxymethyl)-2-methyl-4-oxo-3,4-dihydro-2*H*-chromene-6-carboxylic acid. As compound **7** was obtained as a suitable crystal for an X-ray diffraction, its X-ray analysis was carried out. The ORTEP view of compound **7**, shown in Figure 17, revealed the absolute configuration for C-2 as 2*S*. A literature search revealed that compound **7** is also a new compound, so we named it quadricinctone D.

Table 7. ^1H and ^{13}C NMR ($CDCl_3$, 300.13 MHz and 75.47 MHz) and HMBC assignment for **7**.

Position	δ_C, Type	δ_H, (*J* in Hz)	COSY	HMBC	NOESY
2	80.3, C	-			
3α	434, CH_2	2.74, d (16.7)	H-3	C-2, 4, 10, 11	H_3-11 (str)
β		3.00, d (16.7)	H-3	C-2, 4, 10, 11	H_3-11 (w)
4	191.1, CO	-			
4a	123.0, C	-			
5	127.5, CH	8.26, d (2.3)	H-7	C-4, 7, 8a	
6	119.6, C	-			
7	136.4, CH	8.04, dd (8.7, 2.3)	H-5, 8	C-5, 8a	
8	118.5, CH	7.07, d (8.7)	H-7	C-4a, 6, 8	
8a	162.9, C	-			
9	21.2, CH_3	1.30, s	-	C-2, 3, 10	H-3α (str), H3β (w), H-5, 8 (w)
10	66.8, CH_2	3.49, dd (11.6, 4.5) 3.59, dd (11.6, 4.2)	OH-10		
11	166.4, CO	-			
OH-10	-	5.26, brt (5.4)	-		
OH-11	-	12.69, br	-		

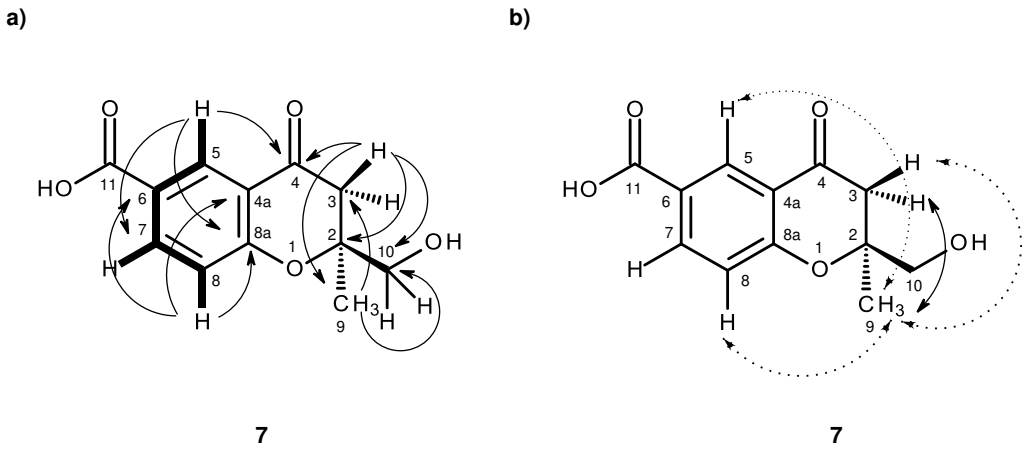

Figure 16. Key COSY (–), HMBC (→) (**a**) and NOESY C-2 (↔) (**b**) C-2 for compound **7**.

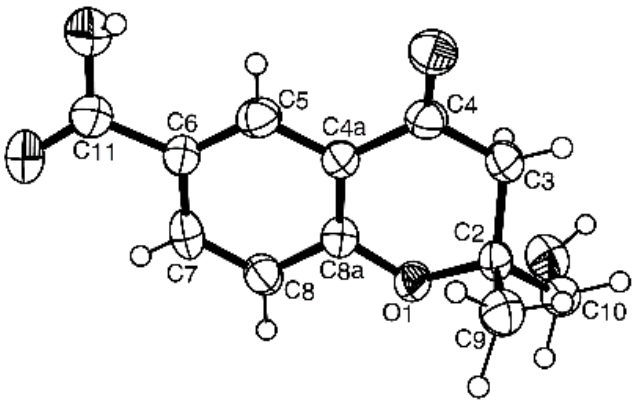

Figure 17. ORTEP diagram of compound **7**.

In order to establish the conformation of the 2,3-dihydro-*4H*-pyran-4-one, analysis of the NOESY correlations was carried out. The NOESY spectrum (Table 7, Figure 16b, Supplementary Information, Figure S52) exhibited not only a strong correlation of H-7 to H-8, but also week correlations of H_3-9 to H-5 and H-8. Therefore, CH_3-9 is in the α-axial position. Additionally, since H_3-9 also exhibited a strong cross-peak with the signal of the methylene proton at δ_H 2.74, d (J = 16.7 Hz), and a weak cross-peak with the proton signal at δ_H 3.00, d (J = 16.7 Hz), the former was assigned to H-3α and the latter to H-3β. It is interesting to observe that the structure of compound **7** is analogous to the structure of compound **3** in that it also exhibits the same methyl-methylene bridge structural feature (at C-9 and C-3), with the same relative intensity of NOESY cross-peaks between the protons of the two groups and with similar conformational energies for the two half-chair conformations of the non-aromatic ring. Therefore, the conclusions drawn for compound **3** are also valid for compound **7**, whose stereochemistry is unequivocally defined by X-ray analysis.

Compounds **1** and **5** can be hypothesized as originating from the pentaketide intermediate (I). Methylation (by SAM) gives II, which undergoes cyclization and enolization to give the intermediate III. Methylation of the phenolic hydroxyl groups and the α-carbon of the carbonyl ketone leads to the intermediate IV. Enolization, followed by a lactonization, originates V, which undergoes hydration to give VI, and oxidation of one of the methyl groups gives rise to compound **5**. Alternatively, oxidation of the α-carbon of the side chain of IV leads to the intermediate VII, which, after lactonization and reduction of the ketone carbonyl, gives rise to compound **1** (Figure 18).

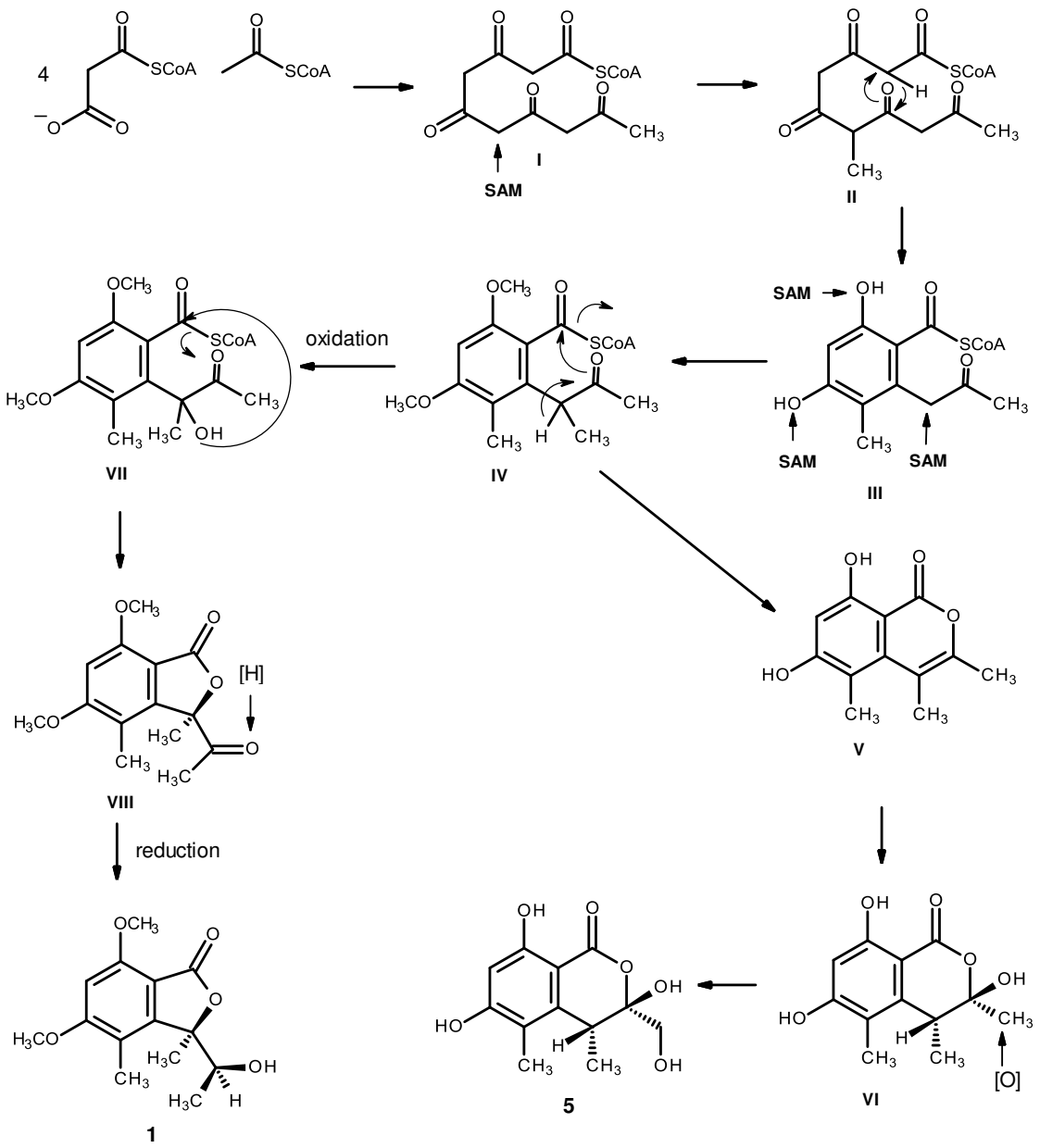

Figure 18. Proposed biosynthetic pathways for compounds **1** and **5**.

Biosynthetically, compounds **2a**, **2b**, **4a**, **4b**, **6a**, **6b** and **7** are of mixed origin, i.e., shikimic acid and mevalonic acid pathways, similar to that proposed for fomannoxin [19], as depicted in Figure 19. Elimination of pyruvate from chorismate (IX) by chorismate pyruvate lyase leads to the formation of *p*-hydroxybenzoic acid (X), which after prenylation by DMAPP (XI), originates the intermediate XII. Epoxidation and cyclization of XII, via Route *a*, leads to a formation of the furan ring in compound **6a** and after oxidation of one of the methyl groups leads to compound **6b**. On the other hand, cyclization via Route *b* leads to the formation of the pyran ring in XIV. Dehydration and oxidation of one of the methyl groups originates compound **2a**, which after acetylation of the primary alcohol function of the side chain will originate compound **2b**. Alternatively, the intermediate XIV can also undergo dehydration, reduction and oxidation to give the ketone function in compound **7**. Oxidative decarboxylation of compound **7** leads to the formation of compound **4a**, which after sulfinylation of the benzene ring originates compound **4b**. However, it is possible that the introduction of the methyl sulfoxide group to the aromatic ring could happen before cyclization.

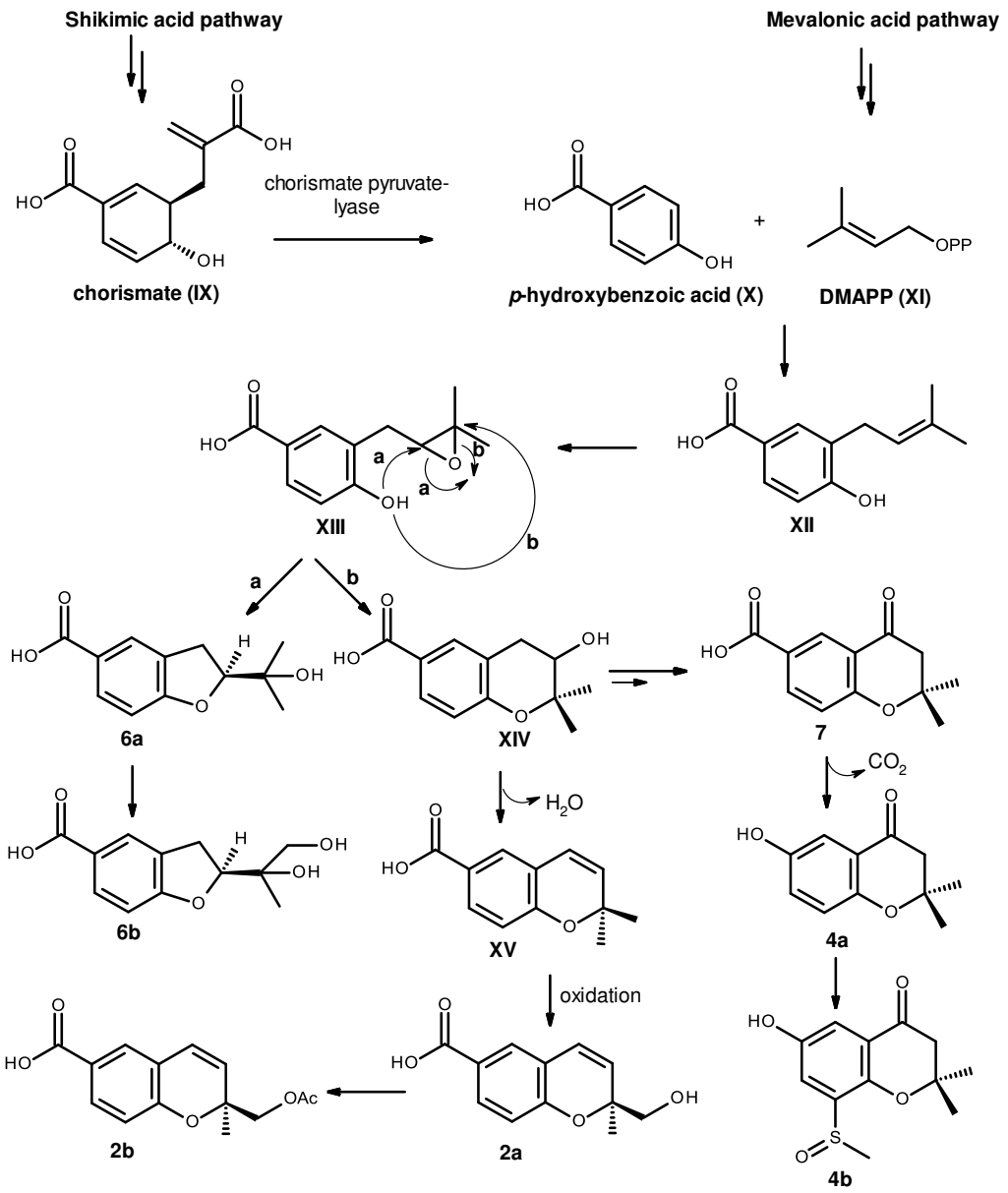

Figure 19. Proposed biosynthetic pathway for compounds **2a**, **2b**, **4a**, **4b**, **6a**, **6b** and **7**.

Compound **3** is also derived from a prenylation of *p*-hydroxybenzoic acid (X); however, it can occur with IPP (XVI) instead of DMAPP (XI). Epoxidation of the double bond of the side chain of XVII, followed by cyclization of XVIII leads to the formation of an oxepin ring in XIX. Oxidation and dehydration of the oxepin ring will lead to the formation of compound **3**, as depicted in Figure 20.

Compounds **1**–**7** were evaluated for their antibacterial activity against Gram-positive and Gram-negative bacteria, as well as multidrug-resistant isolates from the environment, according to the previously described protocol [6], as well as for their antifungal activity against yeast (*Candida albicans* ATCC 10231), filamentous fungus (*Aspergillus fumigatus* ATCC 46645) and dermatophyte (*Trichophyton rubrum* FF5) in the antifungal assay [20]. The results showed that none of the tested compounds exhibited significant antibacterial activity (MIC > 256 μg/mL) or antifungal activity (MIC > 512 μg/mL). These compounds were also evaluated for their in vitro growth inhibitory activity against the MCF-7 (breast adenocarcinoma), NCI-H460 (non-small cell lung cancer) and A375-C5 (melanoma) cell lines by the protein binding dye SRB method [21], and they did not show any activity in this assay (GI_{50} > 150 mM).

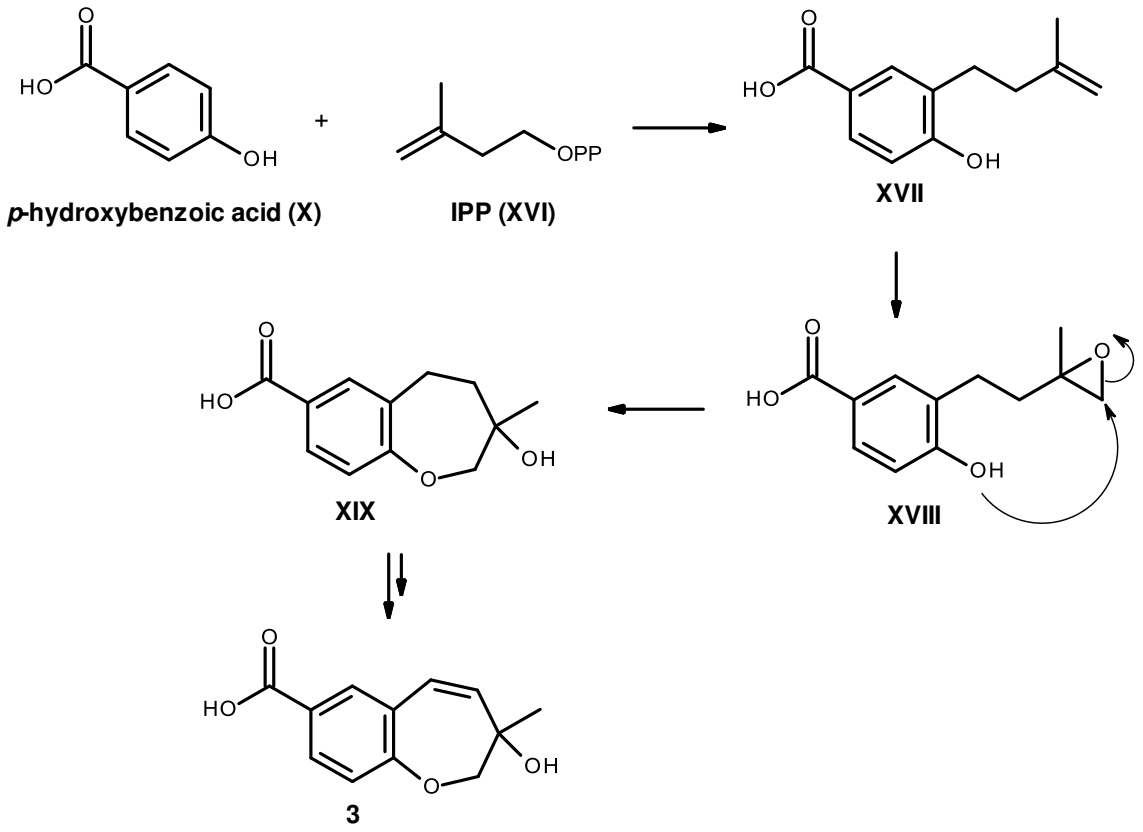

Figure 20. Proposed biosynthetic pathway for compound **3**.

3. Experimental Section

3.1. General Procedure

Melting points were determined on a Bock monoscope and are uncorrected. Optical rotations were measured on an ADP410 Polarimeter (Bellingham + Stanley Ltd., Tunbridge Wells, Kent, U.K.). Infrared spectra were recorded in a KBr microplate in a FTIR spectrometer Nicolet iS10 from Thermo Scientific (Waltham, MA, USA) with the Smart OMNI-Transmission accessory (Software 188 OMNIC 8.3). UV spectra were taken in $CHCl_3$ and were recorded on a Varian CARY 100 spectrophotometer. ^{1}H and ^{13}C NMR spectra were recorded at ambient temperature on a Bruker AMC instrument (Bruker Biosciences Corporation, Billerica, MA, USA) operating at 300.13 and 75.4 MHz, respectively. High resolution mass spectra were measured with a Waters Xevo QToF mass spectrometer (Waters Corporations, Milford, MA, USA) coupled to a Waters Acquity UPLC system. A Merck (Darmstadt, Germany) silica gel GF_{254} was used for preparative TLC, and a Merck Si gel 60 (0.2–0.5 mm) was used for column chromatography.

3.2. Extraction and Isolation

The strain KUFA 0081 was isolated from the marine sponge *Clathria reinwardti*, which was collected, by scuba diving at a depth of 15–20 m, from the coral reef at Samae San Island (12°34′ 36.64″ N 100°56′ 59.69″ E) in the Gulf of Thailand, Chonburi Province, in July 2013. The sponge was washed with 0.06% sodium hypochlorite solution for 1 min, followed by sterilized seawater 3 times and then dried on sterile filter paper, cut into small pieces (5 × 5 mm) and placed on a malt extract agar (MEA) medium containing 70% seawater and 300 mg/L of streptomycin sulphate, then incubated at 28 °C for 7 days, after which the hyphal tips were transferred onto a slant MEA and maintained as pure culture for further identification. The fungus was identified as *Neosartorya quadricincta* (E. Yuill)

Malloch & Cain by one of us (T.D.), based on morphological characteristics, such as colony growth rate and growth pattern on standard media, namely Czapek's agar, Czapek yeast autolysate agar and malt extract agar. Microscopic characteristics, including size, shape and the ornamentation of ascospores, were examined under light and scanning electron microscopes. This identification was supported by sequence analysis of the β-tubulin, calmodulin and actin genes as described in the previous report [22]. *Neosartorya quadricincta* was also confirmed by the analysis sequence of the internal transcribed spacer (ITS) gene according the procedure previously described by us [7]. Its gene sequences were deposited in GenBank with Accession Numbers KM095492 and KT201525, respectively. The pure cultures were deposited as KUFA0081 at Kasetsart University Fungal Collection, Department of Plant Pathology, Faculty of Agriculture, Kasetsart University, Bangkok, Thailand.

The fungus was cultured for one week at 28 °C in 10 Petri dishes (i.d. 90 mm) containing 25 mL of MEA. In order to obtain the mycelial suspension, the mycelial plugs were transferred to two 500-mL Erlenmeyer flasks containing 200 mL of potato dextrose broth and then incubated on a rotary shaker at 120 rpm at 28 °C for 4 days. Fifty 1000-mL Erlenmeyer flasks, each containing 300 g of cooked rice, were autoclaved at 121 °C for 15 min, then inoculated with 20 mL of mycelial suspension of *N. quadricincta* and incubated at 28 °C for 30 days, after which the mouldy rice was macerated in ethyl acetate (25 L total) for 7 days and then filtered. The ethyl acetate solution was concentrated under reduced pressure to yield 176.5 g of crude ethyl acetate extract, which was dissolved in 500 mL of $CHCl_3$ and then washed with H_2O (3 × 500 mL). The organic layers were combined and dried with anhydrous Na_2SO_4, filtered and evaporated under reduced pressure to give 31.1 g of the crude chloroform extract, which was applied on a column of silica gel (440 g) and eluted with mixtures of petrol-$CHCl_3$ and $CHCl_3$-Me_2CO; 250-mL fractions were collected as follows: Frs 1–15 (petrol-$CHCl_3$, 1:1), 16–55 (petrol-$CHCl_3$, 3:7), 56–118 (petrol-$CHCl_3$, 1:9), 119–284 ($CHCl_3$-Me_2CO, 9:1), 285–329 ($CHCl_3$-Me_2CO, 7:1), 330–359 ($CHCl_3$-Me_2CO, 1:1). Frs 175–181 were combined (250 mg) and purified by TLC (silica gel G254, $CHCl_3$-Me_2CO-HCO_2H, 3:2:0.01) to give 86.8 mg of **1** and 15.0 mg of **2b**. Frs 182–197 were combined (565.1 mg) and purified by TLC (silica gel G254, $CHCl_3$-Me_2CO-HCO_2H, 17:3:0.02) to give 35.1 mg of **1** and 14.3 mg of **2b**. Frs 224–235 were combined (249.3 mg) and purified by TLC (silica gel G254, $CHCl_3$-Me_2CO-HCO_2H, 4:1:0.01) to give 11.4 mg of **4a** [12]. Frs 236–285 were combined (1.2 g), applied over a column chromatography of silica gel (42 g) and eluted with mixtures of petrol-$CHCl_3$ and $CHCl_3$-Me_2CO, wherein 100-mL subfractions were collected as follows: sfrs 1–17 (petrol-$CHCl_3$, 1:9), 18–61 ($CHCl_3$-Me_2CO,9:1). Sfrs 24–33 were combined (423.4 mg) and precipitated in a mixture of $CHCl_3$ and Me_2CO to give a white solid (46.2 mg), which was further recrystallized in a mixture of $CHCl_3$ and Me_2CO to give 9.4 mg of white crystals of **6a**, and the mother liquor was purified by TLC (silica gel G254, $CHCl_3$-Me_2CO-HCO_2H, 9:1:0.01) to give 23.2 mg of **6a** and 4.9 mg of **2a**. The mother liquor of sfrs 24–33 (133.0 mg) was purified by TLC (silica gel G254, $CHCl_3$-Me_2CO-HCO_2H, 7: 3:0.01) to give 41.1 mg of **2a** and 12.4 mg of **3**. Sfrs 34–39 were combined (77.7 mg) and purified with TLC (silica gel G254, $CHCl_3$-Me_2CO-HCO_2H, 3: 1:0.01) to give 7.9 mg of **4b** and 17.1 mg of **2a**. Sfrs 40–61 were combined (496.4 mg) and purified by TLC (silica gel G254, $CHCl_3$-Me_2CO-HCO_2H, 4: 1:0.01) to give 22.7 mg of **5**. Frs 307–315 were combined (291.0 mg), applied over a column chromatography of Sephadex LH-20 (10 g) and eluted with a 1:1 mixture of $CHCl_3$: MeOH to give twelve 1-mL sub-fractions. Sfrs 9–12 were combined and purified by TLC (silica gel G254, $CHCl_3$-Me_2CO-HCO_2H, 3: 2:0.01) to give 13.4 mg of **6b** and 9.4 mg of **7**. Frs 316–359 were combined (1.2 g), applied over a column chromatography of Sephadex LH-20 (10 g) and eluted with a 1:1 mixture of $CHCl_3$: MeOH to give twenty-one 1-mL sub-fractions. Sfrs 12–21 were combined (645.7 mg), applied over a column chromatography of Sephadex LH-20 (10 g) and eluted with a 1:1 mixture of $CHCl_3$: MeOH to give sixteen 1-mL fractions. Ssfrs 5–16 were combined (597.5), applied over a column chromatography of silica gel (15 g) and eluted with a mixture of petrol-$CHCl_3$ and $CHCl_3$-Me_2CO, wherein 100-mL fractions were collected as follows: frs 1–8 (petrol-$CHCl_3$, 1:9), 9–28 ($CHCl_3$-Me_2CO, 9:1), 29–41 (($CHCl_3$-Me_2CO, 7:3). Frs 17–18 were combined (47.4 mg) and purified by TLC (silica gel G254, $CHCl_3$-Me_2CO-HCO_2H, 3: 2:0.01) to give 20.8 mg of **6b**.

3.2.1. Quadricinctone A: 3-(1-Hydroxyethyl)-5,7-dimethoxy-3,4-dimethyl-2-benzofuran-1(3*H*)-one (**1**)

White crystals; mp 176–177 °C (petrol/$CHCl_3$); $[\alpha]_D^{20}$ −59° (*c* 0.05, $CHCl_3$); UV (MeOH) λ_{max} (log ε) 233 (4.39), 260 (4.03), 298 (3.78) nm; IR (KBr) υ_{max} 3455, 2981, 2490, 1723, 1612, 1596, 1499, 1467, 1432, 1228 cm^{-1}; ^1H and ^{13}C NMR, see Table 1; HRESIMS *m/z* 267.1243 $[M + H]^+$ (calculated for $C_{14}H_{19}O_5$, 267.1332).

3.2.2. Quadricinctapyran A: 2-(Hydroxymethyl)-2-methyl-2*H*-chromene-6-carboxylic acid (**2a**)

White crystals; mp 147–148 °C ($CHCl_3$/Me_2CO); $[\alpha]_D^{20}$ +30° (*c* 0.03, MeOH); UV (MeOH) λ_{max} (log ε) 237 (4.61) nm; IR (KBr) υ_{max} 3447, 2922, 2359, 2341, 1696, 1647, 1609, 1578, 1490, 143, 1301, 1267 cm^{-1}; ^1H and ^{13}C NMR, see Table 2; HRESIMS *m/z* 221.0820 $[M + H]^+$ (calculated for $C_{12}H_{13}O_4$, 221.0814).

3.2.3. Quadricinctapyran B: 2-[(Acetyloxy)methyl]-2-methyl-2*H*-chromene-6-carboxylic acid (**2b**).

White solid; mp 118–119 °C (petrol/$CHCl_3$); $[\alpha]_D^{20}$ +58° (*c* 0.07, $CHCl_3$); UV (MeOH) λ_{max} (log ε) 201 (4.13), 237 (4.47) nm; IR (KBr) υ_{max} 3441, 2986, 2943, 1745, 1678, 1640, 1607, 1574, 1453, 1419, 1297, 1264, 1228 cm^{-1}; ^1H and ^{13}C NMR, see Table 2; HRESIMS *m/z* 263.0971 $[M + H]^+$ (calculated for $C_{14}H_{15}O_5$, 263.0919).

3.2.4. Quadricinctoxepine: 3-Hydroxy-3-methyl-2,3-dihydro-1-benzoxepine-7-carboxylic acid (**3**)

White solid; mp 189–191 °C ($CHCl_3$/Me_2CO); $[\alpha]_D^{20}$ +21° (*c* 0.07, MeOH); UV (MeOH) λ_{max} (log ε) 234 (4.50) nm; IR (KBr) υ_{max} 3404, 2921, 2359, 2342, 1701, 1606, 1574, 1497, 1384, 1297, 1259, 1117 cm^{-1}; ^1H and ^{13}C NMR, see Table 3; HRESIMS *m/z* 221.0819 $[M + H]^+$ (calculated for $C_{12}H_{13}O_4$, 221.0814).

3.2.5. Quadricinctone B: 6-Hydroxy-2,2-dimethyl-8-(methylsulfinyl)-2,3-dihydro-4*H*-chromen-4-one (**4b**)

White crystals; mp 227–228 °C ($CHCl_3$/Me_2CO); $[\alpha]_D^{20}$ +30° (*c* 0.03, MeOH); UV (MeOH) λ_{max} (log ε) 205 (4.27), 234 (4.22), 358 (3.64) nm; IR (KBr) υ_{max} 3442, 2975, 2922, 1690, 1622, 1484, 1441, 1417, 1326, 1251, 1177 cm^{-1}; ^1H and ^{13}C NMR, see Table 4; HRESIMS *m/z* 255.0694 $[M + H]^+$ (calculated for $C_{12}H_{15}O_4S$, 255.0691).

3.2.6. Quadricinctone C: 3,6,8-Trihydroxy-3-(hydroxymethyl)-4,5-dimethyl-3,4-dihydro-1*H* -isochromen-1-one (**5**)

White crystals; mp 223–224 °C ($CHCl_3$/Me_2CO); $[\alpha]_D^{20}$ +64° (*c* 0.06, MeOH); UV (MeOH) λ_{max} (log ε) 214 (4.23), 271 (3.96), 312 (3.70) nm; IR (KBr) υ_{max} 3439, 3006, 2976, 2360, 2342, 1660, 1644, 1600, 1494, 1472, 1448, 1385, 1157 cm^{-1}; ^1H and ^{13}C NMR, see Table 5; HRESIMS *m/z* 255.0875 $[M + H]^+$ (calculated for $C_{12}H_{15}O_6$, 255.0869).

3.2.7. Quadricinctafuran A: (2*R*)-(2-Hydroxypropan-2-yl)-2,3-dihydro-1-benzofuran-5-carboxylic acid (**6a**)

White crystals; mp 149–150 °C ($CHCl_3$/Me_2CO); $[\alpha]_D^{20}$ +74° (*c* 0.03, MeOH); UV (MeOH) λ_{max} (log ε) 203 (3.40), 254 (3.49) nm; IR (KBr) υ_{max} 3417, 2920, 1681, 1634, 1491, 1261 cm^{-1}; ^1H and ^{13}C NMR, see Table 6; HRESIMS *m/z* 223.9067$[M + H]^+$ (calculated for $C_{12}H_{15}O_4$, 223.0970).

3.2.8. Quadricinctafuran B: (2R)-2-(1,2-Hihydroxypropan-2-yl)-2,3-dihydro-1-benzofuran-5-carboxylic acid (**6b**)

White solid; mp 209–210 °C ($CHCl_3$/Me_2CO); $[\alpha]_D^{20}$ +20° (*c* 0.05, MeOH); UV (MeOH) λ_{max} (log ε) 205 (4.27), 261 (4.03) nm; IR (KBr) υ_{max} 3328, 2984, 2941, 1673, 1610, 1599, 1495, 1362, 1290, 1247 cm^{-1}; ^1H and ^{13}C NMR, see Table 6; HRESIMS *m/z* 239.0919$[M + H]^+$ (calculated for $C_{12}H_{15}O_5$, 239.0919).

3.2.9. Quadricinctone D: 7-Hydroxy-3-(hydroxymethyl)-3-methyl-3,4-dihydro-2-benzoxepine-1, 5-dione (**7**)

White crystals; mp 196–197 °C ($CHCl_3$/Me_2CO); $[\alpha]_D^{20}$ +19° (*c* 0.05, MeOH); UV (MeOH) λ_{max} (log ε) 232 (4.21), 254 (3.84) nm; IR (KBr) υ_{max} 3404, 2934, 2360, 2341, 1708, 1670, 1614, 1492,

1466, 1250 cm^{-1}; ^{1}H and ^{13}C NMR, see Table 7; HRESIMS *m/z* 237.0792 $[M + H]^+$ (calculated for $C_{12}H_{15}O_5$, 237.0763).

*3.3. X-Ray Crystal Structure of Compounds **1**, **2a**, **4b**, **5**, **6a** and **7***

Diffraction data were collected at 293 K with a Gemini PX Ultra equipped with CuK_α radiation (λ = 1.54184 Å). The structures were solved by direct methods using SHELXS-97 and refined with SHELXL-97 [23]. Carbon, oxygen and sulphur atoms were refined anisotropically. Hydrogen atoms were either placed at their idealized positions using appropriate HFIX instructions in SHELXL and included in subsequent refinement cycles or were directly found from difference Fourier maps and were refined freely with isotropic displacement parameters. Full details of the data collection and refinement and tables of atomic coordinates, bond lengths and angles and torsion angles have been deposited with the Cambridge Crystallographic Data Centre.

Quadricinctone A (**1**): Crystals were triclinic, space group P1, cell volume 663.27(7) $Å^3$ and unit cell dimensions a = 7.3973(5)Å, b =8.4830(6)Å and c = 11.2438(6) Å and angles α = 107.541(5)°, β = 92.005(5)° and γ = 98.365(6)° (uncertainties in parentheses). The refinement converged to R (all data) = 3.68% and wR_2 (all data) = 9.54%. The absolute structure was established with confidence (flack x parameter 0.028(18)). CCDC 1465376.

Quadricinctapyran A (**2a**): Crystals were orthorhombic, space group P*bcn*, cell volume 2189.45(9) $Å^3$ and unit cell dimensions a = 21.3981(5)Å, b = 14.5017(3)Å and c = 7.05561(18)Å. The refinement converged to R (all data) = 15.06% and wR_2 (all data) = 40.39%. CCDC 1468869.

Quadricinctone B (**4b**): Crystals were orthorhombic, space group I*ba*2, cell volume 2469.66(11) $Å^3$ and unit cell dimensions a = 8.52510(19)Å, b = 30.2340(7)Å and c = 9.5817(3)Å. The refinement converged to R (all data) = 5.90% and wR_2 (all data) = 15.62%. The absolute structure was established with confidence (flack x parameter −0.04(4)). CCDC 1468868.

Quadricinctone C (**5**): Crystals were monoclinic, space group $P2_1$, cell volume 1116.25(5) $Å^3$ and unit cell dimensions a = 12.1131(3)Å, b = 7.0501(2)Å and c = 13.2091(3)Å and β = 98.291(2)°. The refinement converged to R (all data) = 6.85% and wR_2 (all data) = 17.04%. CCDC 1468170.

Quadricinctafuran A (**6a**): Crystals were monoclinic, space group $P2_1/n$, cell volume 1066.67(10)$Å^3$ and unit cell dimensions a = 11.6064(7)Å, b = 5.9593(2)Å and c = 15.8588(8)Å and β = 103.481(6)°. The refinement converged to R (all data) = 11.08% and wR_2 (all data) = 24.01%. CCDC 1468171.

Quadricinctone D (**7**): Crystals were orthorhombic, space group $Pca2_1$, cell volume 1081.35(13) $Å^3$ and unit cell dimensions a = 19.5607(13)Å, b = 7.4646(5)Å and c = 7.4058(5)Å. The refinement converged to R (all data) = 3.81% and wR_2 (all data) = 8.57%. CCDC 1468166.

*3.4. Molecular Mechanics Conformation Analysis of **3** and **7***

Molecular simulations for Structures **3** and **7** were carried out in ChemBio3D Ultra 14 (Perkin-Elmer). Molecular mechanics energy minimizations used the MM2 and MMFF force fields with the ChemBio3D most recent default parameters and implementation, adequate for small to medium carbon-based models. Ab initio MP2/6-311G and semi-empirical PM3 molecular modelling was done using CS GAMESS interfaced by ChemBio3D. The conformational search was done by stochastic, dihedral driver and molecular dynamics methods. Around 60 conformations were stochastically created and then minimized using the PM3, MMFF and PM3 methods. The resulting models were then grouped under the resultant two seven-membered ring conformations (exemplified in Figure 8 for **3**). A minimal energy for each model set was found by driving by 360° the dihedral angles of the

single bonds that attach substituent groups to the rings. Molecular dynamics runs were also applied to the models to confirm the convergence to a minimal energy conformation for each model set.

4. Conclusions

Although Ozoe et al. had first reported the isolation of an isocoumarin derivative from the culture of the fungus *N. quadricincta* strain PF1223, using a GABA receptor ligand as a screening target, the source of the fungus was not revealed. Therefore, this is the first report on the secondary metabolites of the culture of a marine-derived *N. quadricincta* (KUFA 0081). Among the nine new isolated compounds, two are polyketide derivatives, and seven are benzoic acid derivatives. The isolation of these structurally-unique, but related, metabolites from this fungus has allowed us to propose the biosynthetic pathways leading to these metabolites. Interestingly, the unprecedented structure of quadricinctone B (**4b**), which possesses a methyl sulfinyl group in the benzopyran nucleus, reflects the capacity of this marine-derived strain to introduce sulphur into the aromatic ring. Therefore, this marine strain of *N. quadricincta* (KUFA 0081) can have potential for biotechnological transformation. Even though the isolated metabolites did not exhibit either antifungal/antibacterial activities or growth inhibitory activity against the three cancer cell lines in our assay protocols, it does not mean that they are devoid of other interesting biological activities. Therefore, it is necessary to investigate these metabolites in other target-based assay protocols.

Supplementary Materials: The supplementary materials are available online at www.mdpi.com/1660-3397/14/7/134/s1.

Acknowledgments: This work was developed in the Natural Products Research Laboratory of the Department of Chemistry, Instituto de Ciências Biomédicas Abel Salazar (ICBAS), of the University of Porto and partially supported through national funds provided by FCT-Foundation for Science and Technology and European Regional Development Fund (ERDF) and COMPETE, under the projects PEst-C/MAR/LA0015/2013, PTDC/MAR-BIO/4694/2014, as well as by the project INNOVMAR (Innovation and Sustainability in the Management and Exploitation of Marine Resources) (Reference NORTE-01-0145-FEDER-000035, within Research Line NOVELMAR/INSEAFOOD/ECOSERVICES), supported by the North Portugal Regional Operational Programme (NORTE 2020), under the PORTUGAL 2020 Partnership Agreement, through the European Regional Development Fund (ERDF). We thank Mrs. Júlia Bessa and Sara Cravo for technical support.

Author Contributions: A. Kijjoa and M. Pinto conceived, designed the experiments and wrote the paper; C. Prompanya performed isolation and purification of the compounds; T. Dethoup collected, isolated, identified and cultured the fungus; L. Gales performed X-ray analysis; J. Pereira performed molecular mechanics conformation analysis; A. Silva provided NMR spectra; M. Lee provided HRMS.

Conflicts of Interest: The authors declare no conflict of interest.

References

1. Hong, S.-B.; Shin, H.-D.; Hong, J.; Frisvad, J.C.; Nielsen, P.V.; Varga, J.; Samson, R.A. New taxa of *Neosartorya* and *Aspergillus* in *Aspergillus* section Fumigati. *Antonie Van Leeuwenhoek* **2008**, *93*, 87–98. [CrossRef] [PubMed]
2. Kijjoa, A.; Santos, S.; Dethoup, T.; Manoch, L.; Almeida, A.P.; Vasconcelos, M.H.; Silva, A.; Gales, L.; Herz, W. Sartoryglabrins, Analogs of the Ardeemins from *Neosartorya glabra*. *Nat. Prod. Commun.* **2011**, *6*, 807–812. [PubMed]
3. Eamvijarn, A.; Anake Kijjoa, A.; Bruyère, C.; Mathieu, V.; Manoch, L.; Lefranc, F.; Silva, A.; Kiss, R.; Herz, W. Secondary Metabolites from a Culture of the Fungus *Neosartorya pseudofischeri* and Their in Vitro Cytostatic Activity in Human Cancer Cells. *Planta Med.* **2012**, *28*, 167–176. [CrossRef] [PubMed]
4. Buttachon, S.; Chandrapatya, A.; Manoch, L.; Silva, A.; Gales, L.; Bruyére, C.; Kiss, R.; Kijjoa, A. Sartorymensin, a New Indole Alkaloid, and New Analogues of Tryptoquivaline and Fiscalins Produced by *Neosartorya siamensis* (KUFC 6349). *Tetrahedron* **2012**, *68*, 3253–3262. [CrossRef]
5. Eamvijarn, A.; Gomes, N.M.; Dethoup, T.; Buaruang, J.; Manoch, L.; Silva, A.; Pedro, M.; Marini, I.; Roussis, V.; Kijjoa, A. Bioactive Meroditerpenes and Indole Alkaloids from the Soil Fungus *Neosartorya fischeri* (KUFC 6344) and the Marine-derived Fungi *Neosartorya laciniosa* (KUFC 7896) and *Neosartorya tsunodae* (KUFC 9213). *Tetrahedron* **2013**, *69*, 8583–8591. [CrossRef]

6. Gomes, N.M.; Bessa, L.J.; Buttachon, S.; Costa, P.M.; Buaruang, J.; Dethoup, T.; Silva, A.M.S.; Kijjoa, A. Antibacterial and Antibiofilm Activity of Tryptoquivalines and Meroditerpenes from Marine-Deived Fungi *Neosartorya paulistensis*, *N. laciniosa*, *N. tsunodae,* and the soil fungi *N. fischeri* and *N. siamensis*. *Mar. Drugs* **2014**, *12*, 822–839. [CrossRef] [PubMed]
7. May Zin, W.W.; Buttachon, S.; Buaruang, J.; Gales, L.; Pereira, J.A.; Pinto, M.M.M.; Silva, A.M.S.; Kijjoa, A. A New Meroditerpene and a New Tryptoquivaline from the Algicolous Fungus *Neosartorya takakii* KUFC 7898. *Mar. Drugs* **2015**, *13*, 3776–3790. [CrossRef] [PubMed]
8. Prompanya, C.; Dethoup, T.; Bessa, L.J.; Pinto, M.M.M.; Gales, L.; Costa, P.M.; Silva, A.M.S.; Kijjoa, A. New Isocoumarin Derivatives and Meroterpenoids from the Marine Sponge-Associated Fungus *Aspergillus similanensis* sp. nov. KUFA 0013. *Mar. Drugs* **2014**, *12*, 5160–5173. [CrossRef] [PubMed]
9. Prompanya, C.; Fernandes, C.; Cravo, S.; Pinto, M.M.; Dethoup, T.; Silva, A.M.; Kijjoa, A. A New Cyclic Hexapeptide and a New Isocoumarin Derivative from the Marine Sponge-Associated Fungus *Aspergillus similanensis* KUFA 0013. *Mar. Drugs* **2015**, *13*, 1432–1450. [CrossRef] [PubMed]
10. Boonsang, N.; Dethoup, T.; Singburaudom, N.; Gomes, N.G.M.; Kijjoa, A. In Vitro Antifungal Activity Screening of Crude Extracts of Soil Fungi against Plant Pathogenic Fungi. *J. Biopest.* **2014**, *7*, 156–166.
11. Ozoe, Y.; Kuriyama, T.; Tachibana, Y.; Harimaya, K.; Takahashi, N.; Yaguchi, T.; Suzuki, E.; Imamura, K.; Oyama, K. Isocoumarin Derivative as a Novel GABA Receptor Ligand from *Neosartorya quadricincta*. *J. Pestic. Sci.* **2004**, *29*, 328–331. [CrossRef]
12. Lourenço, T.O.; Akisue, G.; Roque, N.F. Reduced Acetophenone Derivatives from *Calea cuneifolia*. *Phytochemistry* **1981**, *20*, 773–776. [CrossRef]
13. Fletcher, C.M.; Jones, D.N.M.; Diamond, R.; Neuhaus, D. Treatment of NOE constraints involving equivalent or nonstereoassigned protons in calculations of biomolecular structures. *J. Biomol. NMR* **1996**, *8*, 292–310. [CrossRef] [PubMed]
14. Butts, C.P.; Jones, C.R.; Towers, E.C.; Flynn, J.L.; Appleby, L.; Barron, N. Interproton distance determinations by NOE—Surprising accuracy and precision in a rigid organic molecule. *J. Org. Biomol. Chem.* **2011**, *9*, 177–184. [CrossRef] [PubMed]
15. Shima, K.; Hisada, S.; Inagaki, I. Studies on the constituents of *Anodendron affine* Durce. V. Isolation and structure of two new constituents. *Yakugaku Zasshi* **1972**, *92*, 1410–1414. [PubMed]
16. Yamaguchi, S.; Kondo, S.; Shimokawa, K.; Inoue, O.; Sannomiya, M.; Kawase, Y. The synthesis of racemic fomannoxin, anodendroic acid, and 5-acetyl-2-[1-(hydroxymethyl)vinyl]-2,3-dihydrobenzofuran. *Bull. Chem. Soc. Jpn.* **1982**, *55*, 2500–2503. [CrossRef]
17. Arriaga-Giner, F.J.; Wollenweber, E.; Schober, I.; Yatskievych, G. Three New Benzoic Acid Derivatives from the Glandular Excretion of *Eriodictyon sessilifolium* (Hydrophyllaceae). *Z. Naturforch.* **1988**, *43c*, 337–340.
18. Bisogno, F.; Mascoti, L.; Sanchez, C.; Garibotto, F.; Giannini, F.; Kurina-Sanz, M.; Enriz, R. Structure-antifungal activity relationship of cinnamic acid derivatives. *J. Agric. Food Chem.* **2007**, *55*, 10635–10640. [CrossRef] [PubMed]
19. Hansson, D.; Menkis, A.; Olson, Å.; Stenlid, J.; Broberg, A.; Karlsson, M. Biosynthesis of fomannoxin in the root rotting pathogen *Heterobasidion occidentale*. *Phytochemistry* **2012**, *84*, 31–39. [CrossRef] [PubMed]
20. Wattanadilok, R.; Sawangwong, P.; Rodrigues, C.; Cidade, H.; Pinto, M.; Pinto, E.; Silva, A.; Kijjoa, A. Antifungal activity evaluation of the constituents of *Haliclona baeri* and *H. cymaeformis*, collected from the Gulf of Thailand. *Mar. Drugs* **2007**, *5*, 40–51. [CrossRef] [PubMed]
21. Cidade, H.M.; Nascimento, M.S.J.; Pinto, M.M.M.; Kijjoa, A.; Silva, A.M.S.; Herz, W. Artelastocarpin and carpelastofuran, two new flavones, and cytotoxicities of prenyl flavonoids from *Artocarpus elasticus* against three cancer cell lines. *Planta Med.* **2001**, *67*, 867–870. [CrossRef] [PubMed]
22. Matsuzawa, T.; Horie, Y.; Abliz, P.; Gonoi, T.; Yaguchi, T. *Aspergillus huiyaniae* sp. nov., a new teleomorphic species in Aspergillus section *Fumigati* isolated from desert soil in China, and described using polyphasic approach. *Mycoscience* **2014**, *55*, 213–220. [CrossRef]
23. Sheldrick, G.M.A. A short history of SHELX. *Acta Cryst.* **2008**, *A64*, 112–122. [CrossRef] [PubMed]

© 2016 by the authors; licensee MDPI, Basel, Switzerland. This article is an open access article distributed under the terms and conditions of the Creative Commons Attribution (CC-BY) license (http://creativecommons.org/licenses/by/4.0/).